EVALUATION OF PROPAGATION SENSITIVITY OF COMMERCIAL EXPLOSIVES IN 15 CM DIAMETER HOLES

FINAL REPORT

CONTRACT NO. 0SQ85-00238
FC: 230-131-000000-110702-0415
DSS FILE NO. 07SQ.23440-5-9081

SUBMITTED TO:

R.R. VANDEBEEK
CANMET - MINING RESEARCH LABORATORIES

SUBMITTED BY:

A.W. BAUER

SUPERVISOR: A. BAUER

MINING RESOURCE ENGINEERING LIMITED
8 PRINCESS STREET
KINGSTON, ONTARIO
K7L 1A2

MICROMEDIA

122 pp

NOVEMBER 1986

SUMMARY

An investigation was made of the insitu sand gap sensitivity of several commercial explosives. These explosives were tested in granite holes of 90 mm and 150 mm diameter. The "Up-and-Down" statistical method was used to calculate the sand gap distance at which the probability of cross-propagation was 50% and to estimate the distances at 5% and 95% probability of cross-propagation. Both donor and receptor charges were instrumented to indicate initiation or failure of the receptor charge.

AN/FO appears to be more sensitive to initiation through a sand gap than the other products tested. However, AN/FO alone as a receptor charge did not detonate at sand gap distances known to be frequently cross-propagated in mining operations

Subsequent testing with a blasting cap and primer in the receptor charge increased the sand gap distance cross-propagated for one of the products.

This paper provides sand gap performance data for several commercial explosives. It also indicates that the cross-propagation distance between explosive decks in mining situations depends to a great extent on the shock sensitivity of the detonator in the subsequent deck.

SOMMAIRE

La sensibilité des lacunes de sable in situ de plusieurs explosifs a fait l'objet d'études. On a mis à l'essai ces explosifs dans les trous de mine en granit ayant un diamètre de 90 mm et de 150 mm. On a employé la méthode statistique "haute et basse" pour estimer la distance de lacunes de sable à laquelle la probabilité de la propagation croisée était 50% et pour déterminer les distances à une probabilité d'une propagation croisée de 5% et de 95%. On a doté les charges donneuses et réceptrices d'appareils de contrôle automatiques afin d'indiquer l'initiation ou l'échec de la charge réceptrice.

La combinaison d'agents de tir-le nitrate d'ammonium et le pétrole combustible (NO/PC) paraît être plus sensible à l'initiation à travers une lacune de sable que les autres produits mis à l'essai. Cependant, l'emploi de NO/PC comme la seule charge réceptrice ne détone pas aux mêmes distances de lacunes de sable où la propagation croisée est fréquemment observé dans l'exploitation minière.

Les essais suivants utilisant une amorce et une cartouche-amorce dans la charge réceptrice a augmenté la distance de lacune de sable propagée réciproquement pour un des produits.

Cet article fournit les données sur le rendement des lacunes de sable pour plusieurs explosifs commerciaux. Il signale aussi que dans les situations minières la distance de propagation croisée entre les parties constituantes de la charge dépend en grande mesure de la sensibilité au choc du détonateur dans la partie de la charge qui suit.

TABLE OF CONTENTS

		PAGE
	LIST OF FIGURES	vi
	LIST OF TABLES	viii
	CHAPTER 1 - INTRODUCTION TO PROPAGATION SENSITIVITY	
1.0	PROPAGATION SENSITIVITY IN MINING APPLICATIONS.	1
	1.1 BACKGROUND	7
	CHAPTER 2 - DETONATION THEORY RELEVANT TO EXPLOSIVE SENSITIVITY	
2.0	INTRODUCTION	11
	2.1 INITIATION THEORY	12
	2.1.1 Initiation in Solid and Liquid Explosives	13
	2.1.2 Initiation in Explosives Sensitized with Hollow Glass Microbubbles	30
	2.2 PARAMETERS AFFECTING DETONATION	31
	2.2.1 Detonation Head Model	32
	2.2.2 Influence of Confinement	36
	2.2.3 Influence of Temperature Reduction on Explosive Sensitivity	37
	2.2.4 Influence of Static Pressures on Explosive Sensitivity	38
	2.2.5 Influence of Dynamic Pressures on Explosive Sensitivity	40
	2.2.6 Influence of the Gap Material Type on the Propagation of Detonation Across a Gap	42

CHAPTER 3 - EXPERIMENTAL DESIGN AND INSTRUMENTATION

3.0 INTRODUCTION..... 45

3.1 THE GRAPHICAL SOLUTION..... 46

3.2 THE "UP-AND-DOWN" METHOD..... 49

3.2.1 "Up-and-Down" - Example 1..... 55

3.2.2 "Up-and-Down" - Example 2..... 56

3.3 MONITORING THE DONOR AND RECEPTOR CHARGES. 58

CHAPTER 4 - EXPERIMENTAL

4.0 INTRODUCTION..... 63

4.1 SAND GAP TESTS FOR NON-CAP SENSITIVE PRODUCTS A, B, C AND AN/FO..... 65

4.2 SAND GAP TESTS FOR NON-CAP SENSITIVE PRODUCT C WHEN THE RECEPTOR CHARGE CONTAINS A BLASTING CAP AND/OR CAST PRIMER 73

4.3 SAND GAP TESTS FOR CAP SENSITIVE PRODUCT D..... 75

CHAPTER 5 - CONCLUSIONS 82

REFERENCES 84

APPENDIX A: SAMPLE CALCULATION OF THE FINAL TEMPERATURE REACHED IN NON-GASSED NITROMETHANE UNDER SHOCK..... 87

APPENDIX B: SAMPLE CALCULATION OF THE FINAL TEMPERATURE REACHED IN AN AIR BUBBLE UNDER SHOCK..... 91

APPENDIX C: ILLUSTRATION OF CALCULATING THE DONOR CHARGE VELOCITY OF DETONATION..... 93

APPENDIX D: TRADE NAMES OF THE EXPLOSIVES TESTED..... 95 (Removed)

APPENDIX E: "UP-AND-DOWN" RECEPTOR RESULT PLOTS FOR 90 MM DIAMETER PRODUCT A, B, C AND AN/FO CHARGES..... 97

APPENDIX F: "UP-AND-DOWN" RECEPTOR RESULT PLOTS FOR 150 MM DIAMETER PRODUCT A, B, C AND AN/FO CHARGES..... 102

APPENDIX G: "UP-AND-DOWN" RECEPTOR RESULT PLOTS FOR 90 MM AND 150 MM DIAMETER PRODUCT C WITH BLASTING CAP AND CAST PRIMER IN THE RECEPTOR CHARGE..... 107

APPENDIX H: "UP-AND-DOWN" RECEPTOR RESULT PLOTS FOR 50 MM, 90 MM AND 150 MM DIAMETER CAP SENSITIVE PRODUCT D.. 110

LIST OF FIGURES

FIGURE #		PAGE
1	CONTINUOUS EXPLOSIVE CARTRIDGE LOADING OF HORIZONTAL AND VERTICAL HOLES.....	2
2	ILLUSTRATION OF AIR, WATER AND DRILL CUTTING GAPS BETWEEN EXPLOSIVE CARTRIDGES..	4
3	ILLUSTRATION OF A SAND DECKED HOLE.....	5
4	DETONATION PROCESS IN A CYLINDRICAL LIQUID EXPLOSIVE SENSITIZED BY ENTRAPPED AIR BUBBLES.....	33
5	DETONATION PROCESS IN A CYLINDRICAL LIQUID EXPLOSIVE SENSITIZED BY GLASS MICROBUBBLES.	35
6	GRAPHICAL REPRESENTATION OF SAMPLE DATA....	48
7	BLAST MONITORING SYSTEM.....	60
8	DETERMINATION OF RECEPTOR DETONATION OR FAILURE USING THE PROBE CABLE METHOD.....	62
9	CROSS SECTION OF A 90 MM DIAMETER TEST HOLE.....	66
10	CROSS SECTION OF A 150 MM DIAMETER TEST HOLE.....	67
11	SAND GAP DISTANCE VERSUS CHARGE DIAMETER FOR NON-CAP SENSITIVE PRODUCTS AT 50% PROBABILITY OF CROSS-PROPAGATION.....	70
12	SAND GAP DISTANCE VERSUS CHARGE DIAMETER FOR NON-CAP SENSITIVE PRODUCTS AT AN ESTIMATED 95% PROBABILITY OF CROSS-PROPAGATION.....	71
13	SAND GAP DISTANCE VERSUS CHARGE DIAMETER FOR NON-CAP SENSITIVE PRODUCTS AT AN ESTIMATED 5% PROBABILITY OF CROSS-PROPAGATION.....	72
14	CROSS SECTION OF A TEST HOLE ILLUSTRATING THE BLASTING CAP AND PRIMER POSITION IN THE RECEPTOR CHARGE.....	74

15 SAND GAP DISTANCE VERSUS CHARGE DIAMETER FOR NON-CAP SENSITIVE PRODUCT C ILLUSTRATING THE EFFECT OF PLACING A BLASTING CAP AND A CAST PRIMER IN THE RECEPTOR CHARGE..... 77

16 CROSS SECTION OF A 50 MM DIAMETER TEST HOLE..... 78

17 SAND GAP DISTANCE VERSUS CHARGE DIAMETER FOR PRODUCT C AND D AND ON EXTRAPOLATION FROM THE 1985 REPORT(1)..... 81

LIST OF TABLES

TABLE #		PAGE
1	RESULTS OF CALCULATION OF T_{2n}, FINAL TEMPERATURE OF NON-GASSED NITROMETHANE, FOR VARIOUS SHOCK VELOCITIES.....	25
2	COMPARISON OF FINAL TEMPERATURES AND RATIO OF ABSOLUTE REACTION RATES FOR GASSED AND NON-GASSED NITROMETHANE.....	27
3	HYPOTHETICAL DATA FOR AN ILLUSTRATION OF THE GRAPHICAL METHOD[4].....	47
4	TABLE USED IN THE CALCULATION OF THE P50 GAP DISTANCE FOR N LESS THAN OR EQUAL TO SIX[4].....	52
5	TABLE USED IN THE CALCULATION OF THE P50 GAP DISTANCE FOR N GREATER THAN SIX[4].....	54
6	THE EXPLOSIVES AND DIAMETERS TESTED.....	64
7	SAND GAP DISTANCES FOR NON-CAP SENSITIVE PRODUCTS CALCULATED AT 50% AND ESTIMATED FOR 5 AND 95% PROBABILITY OF CROSS-PROPAGATION.....	68
8	SAND GAP DISTANCES FOR PRODUCT C CALCULATED AT 50% AND ESTIMATED FOR 5 AND 95% PROBABILITY OF CROSS-PROPAGATION.....	76
9	SAND GAP DISTANCES FOR PRODUCTS C AND D CALCULATED AT 50% AND ESTIMATED FOR 5 AND 95% PROBABILITY OF CROSS-PROPAGATION.....	79

CHAPTER 1

INTRODUCTION TO PROPAGATION SENSITIVITY

1.0 PROPAGATION SENSITIVITY IN MINING APPLICATIONS

A typical mining or civilian rock blasting situation calls for numerous explosive cartridges to be loaded into a series of horizontal or vertical boreholes as shown in Figure 1. Detonation of these confined lengths of explosive cartridges is achieved through a blasting cap/primer placed in the bottom cartridge of each hole. Detonation of all of the explosive cartridges in a hole relies on the ability of one explosive cartridge, upon detonation, to initiate detonation in its adjacent explosive cartridge and so on.

If the propagation of detonation is stopped in one or more holes, the blast will not perform as expected and rock fragmentation will suffer.

Also when propagation of detonation is stopped some explosive remains undetonated and will eventually be found in the broken rock pile. Digging broken rock mixed with undetonated explosives is a serious safety hazard.

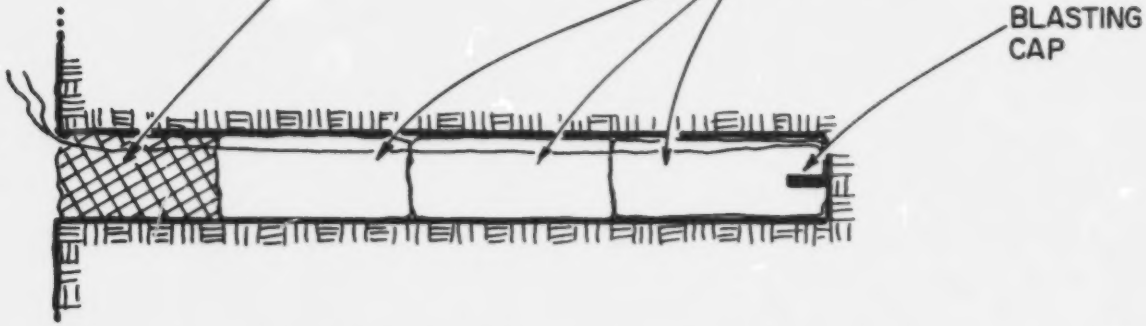

CARTRIDGES IN HORIZONTAL BOREHOLE.

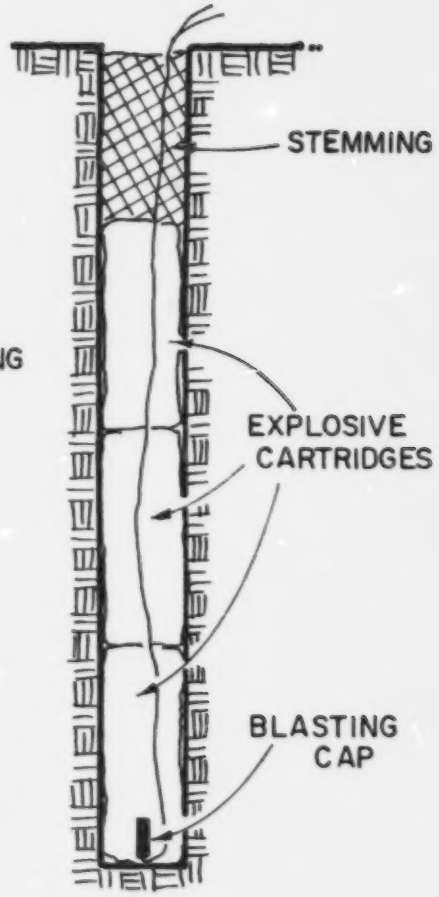

CARTRIDGES IN VERTICAL BOREHOLE.

FIGURE 1 : CONTINUOUS EXPLOSIVE CARTRIDGE LOADING OF HORIZONTAL AND VERTICAL HOLES.

Propagation from cartridge to cartridge is assured if the cartridges are in direct contact. However, poor loading procedures or poor ground conditions can result in a gap distance of air, water, or drill cuttings between adjacent explosive cartridges as illustrated in Figure 2. These gaps reduce the probability of continuous detonation propagation.

A common method of blasting ore underground is called ring blasting. From underground tunnels known as production drifts, 50 mm holes are drilled in a ring pattern around the drift section. Some of these holes are drilled down, some horizontally and the rest are drilled up and inclined. The holes can be up to 18 m long and the rings are usually separated by a distance of up to 2.5 m along the drift length. A series of rings along a drift are usually all loaded with explosives and the rings are shot with one ring going off at a time.

Loading of the inclined holes when ring blasting can lead to air gaps between cartridges. Also the blast effect from the previous ring detonating can cause the holes in the next ring to become offset thereby creating gaps in the explosive column and affecting that ring's performance.

Other mining situations employing larger diameter blastholes (150 mm) call for the explosive column in a hole to be decked with sand as shown in Figure 3. Decking of the explosive column in a hole can be performed to minimize the vibration from a blast in an underground mining operation. Each deck in a hole is initiated individually with predetermined time intervals

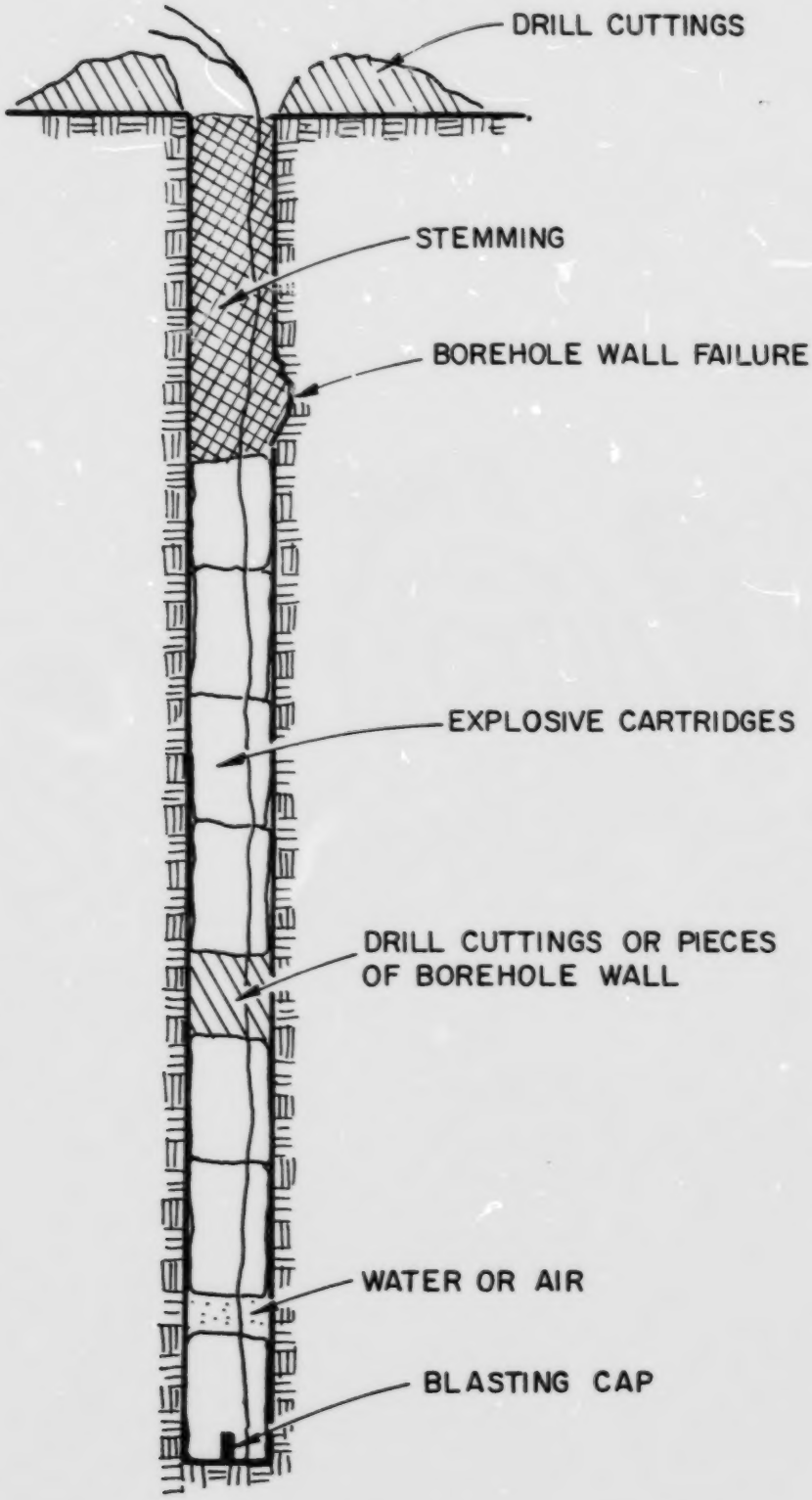

FIGURE 2 : ILLUSTRATION OF AIR, WATER AND DRILL CUTTING GAPS BETWEEN EXPLOSIVE CARTRIDGES.

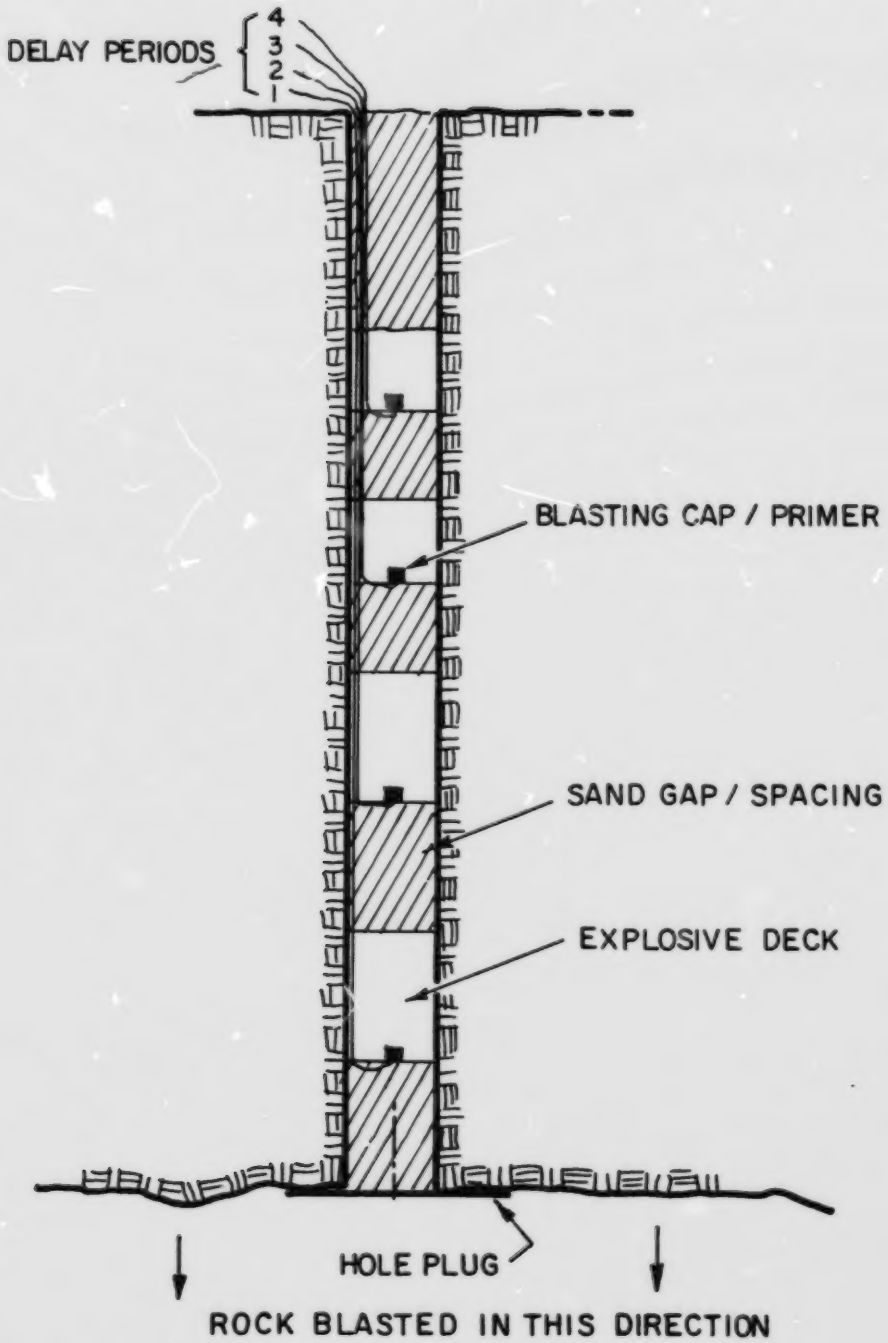

FIGURE 3 : ILLUSTRATION OF A SAND DECKED HOLE .

between decks to regulate the amount of explosive detonating during a given time period. Propagation from one explosive deck to its adjacent explosive deck is not desirable in this case as cross propagation would increase the amount of explosive detonating at one time thereby increasing the ground vibration. This increase in ground vibration can weaken the ground support system in the mine reducing the stability of the underground workings thereby creating hazardous working conditions.

Decking of an explosive column is also performed in some surface blasting operations. Decking in this case is performed to reduce the amount of explosive in each hole. The explosive decks can be separated by air gaps and suspended by spacers in the holes. Generally, only the bottom deck of explosive in each hole is initiated, and cross-propagation of the air gaps is relied upon to initiate subsequent decks in the hole.

It is evident that a very important property of a commercial explosive is the ability of one explosive cartridge or deck to cross-propagate a gap distance of air, sand, or water, and initiate an adjacent explosive cartridge or deck. It is also equally important to be able to determine the distances required to avoid cross-propagation between explosive cartridges or decks. Although laboratory means of estimating propagation sensitivity exist, it is difficult to relate these test results to what actually occurs in a borehole under field conditions.

1.1 BACKGROUND

In a previous study for CANMET (contract no. 0SQ84-00091)[1] field tests were conducted to determine the cross-propagation probability as a function of charge separation distance for hole diameters ranging from 2.5 cm to 5 cm in granite. The effect of infilling material in the gap was studied along with the effect of temperature and degree of decoupling of the donor and receptor charges. An up down technique, similar to the Bruceton method [2,3,4] was used to determine the 50/50 go/no go point for 6 small diameter commercial explosives.

The results indicated that for a particular explosive type, at a given diameter of charge, degree of confinement, and temperature, the distribution of the cross-propagated gap distances around the mean was normal. The development of two experimental distribution curves permitted estimates to be made of the gap distance cross-propagated under given set of test conditions for cross-propagation probabilities of 5, 50 and 95 percent.

The explosive products chosen were sensitized by two different methods. For 2 of the products it was hollow microbubbles whereas for the other 4 products it was entrained gas bubbles used in possible conjunction with liquid chemical sensitizers.

The role of ambient conditions such as temperature could be expected to and did play a significantly greater role in the case of entrained gas sensitization versus microbubble sensitization. If the mechanism of sensitization with hollow low pressure (vacuum) filled microbubbles is from the jet produced when the bubbles collapse then the pressure required to produce high velocity jets from the microbubble collapse can be expected to be high. In other words the cross-propagation gap distances will be small. This will be particularly so with sand filling the gap. The research results showed this to be the case. These results shed valuable insight on the type of loading technique that would have to be used when charging microbubble sensitized explosives into long small diameter boreholes. There was a need for a loading system which would produce essentially a continuous explosive column since for a very high probability of cross-propagation only relatively small air gaps and even smaller sand gaps could be tolerated. For the air bubble sensitized explosives the tolerable gaps were much larger.

In addition to the foregoing and the effects of temperature, degree of coupling etc. the test results permitted the estimation of scaling laws of gap distance as a function of charge diameter at 5, 50 and 95 percent probability of propagation.

In some underground mining applications such as large diameter blast hole stoping it is very important that there not be cross-propagation between deck charges in a particular

borehole. In these applications common sizes of borehole are 90 mm and 150 mm. There is presently no real sound basis for the selection of the sand gap distance to be used between the deck charges. Obviously the separation distance should be short enough to ensure adequate fragmentation from the blast. Often the separation distance in feet of approximately 1.25 to 1.5 times the hole diameter in inches is taken as a rule of thumb to be the minimum gap length to be employed. According to the extrapolated test results from previous test work[1] there is a very high probability of cross-propagation occurring with air bubble sensitized explosives and very low probability of this occurring with microbubble sensitized explosives. Examination of blast vibration records from both surface and underground mines using multideck delayed blasting has also indicated out of sequence firing and the records have been indicative of in hole cross-propagation. Because of this it is usual for explosives manufacturers to use less sensitive formulations for large diameter applications. The products for use in larger diameter boreholes have larger critical diameters and larger minimum primer weight requirements. Therefore the scaling relations determined for small diameter, cap sensitive products may not be applicable to larger diameter situations. It is therefore apparent that typical large diameter products should also undergo sand gap testing.

As an introduction to this research into sand gap cross-propagation phenomena, an overview of detonation theory is detailed as it applies to the gap sensitivity of both air bubble and microbubble sensitized explosive products. Also, the statistical method used to determine the P50 sand gap distances is presented.

The report concludes with presentation and discussion of the test results.

CHAPTER 2

DETONATION THEORY RELEVANT TO EXPLOSIVE SENSITIVITY

2.0 INTRODUCTION

When a condensed explosive suffers a rapid decomposition, the process can be divided into four stages of development. These are initiation, deflagration, transition from deflagration to detonation, and detonation. The process may go to completion or may stop at any stage due to build up or decay of the decomposition rate. Whether decay to failure or build up to detonation occurs depends on the intensity of the initiation stimulus.

In gap sensitivity studies the concern is mainly with the detonation phase of decomposition in the donor charge and the initiation phase of decomposition in the receptor charge. This chapter is presented as a theoretical background on the initiation and detonation process and the factors that will affect detonation in air bubble sensitized and hollow glass sphere, so-called microbubble, sensitized explosives. The concepts presented in this chapter will simplify discussion of the results in the experimental portion of the report.

2.1 INITIATION THEORY

Initiation in condensed explosives is thermal in origin. Mechanical energy must be degraded into heat and concentrated in a small region to form a hot-spot. Thermal ignition of the explosive whether it be solid or liquid then occurs at the hot-spot.

Hot-spots can be formed in three main ways[5]:

1. By the adiabatic compression of small entrapped bubbles of gas.
2. By frictional hot-spots formed: (A) on the confining surfaces, (B) on extraneous grit particles, (C) by intercrystalline friction of explosive particles themselves.
3. By viscous heating of the rapidly flowing explosive as it escapes from between the impacting surfaces.

The third method is operative only under extreme conditions and therefore it is of little importance.[5]

The following sections detail the way in which solid and liquid explosives, some containing voids - some voidless, react to shock energy. References will be made to the work of Bowden and Yoffee[5], Mader[6], Winning[7], and King[8].

2.1.1 Initiation in Solid and Liquid Explosives

When a shock wave travels out from a primer, or in this case a donor charge, the initial effect on the receptor charge is one of compression. If the receptor explosive is either a solid or liquid containing no voids or gas pockets the temperature rise in the compressional wave is not high. This is because both solids and liquids are relatively incompressible. If voids exist in the solid or gas bubbles are entrapped in the liquid then upon shock from the donor charge these voids or bubbles undergo adiabatic compression to a high pressure and hence a high temperature increase occurs.

Mader[6] performed pressure sensitivity tests on both solid and liquid explosives. He found that a single crystal of pentaerythritol tetranitrate, PETN, a monomolecular high explosive with a crystal density of approximately 1.8 g/cc, would detonate only if subjected to a shock pressure of 100 Kbars or greater. When he performed the test on crushed crystals of PETN at a density of 1.0 g/cc, detonation occurred at a shock pressure of 2 Kbars.

Mader found also that it took 2 μsec for normal nitromethane to detonate after it had been subjected to a shock pressure of 85 Kbars. Nitromethane containing air bubbles took 0.1 μsec to reach detonation under the same conditions. Mader also applied 23 Kbars to de-gassed nitromethane to which

grit particles had been added. The time to detonation was 2 μsec in this case. The results of his research indicated that the addition of voids or gas bubbles to solid or liquid explosives increased the sensitivity of explosives. When grit is added to the liquid nitromethane the increase in sensitivity is thought to be due to the reflection and intensification of the shock pressure caused by the significant impedance difference between the grit particle and the liquid.

Bowden and Yoffee[5] performed extensive research into the initiation of liquid and solid explosives. Results of their sensitivity tests on gas bubble sensitized liquid explosives indicated that the sensitivity of the explosive increased with an increase in the value of the ratio of specific heat of the gas forming the bubbles. This supports the view that initiation is due to the adiabatic compression of entrapped gas and the specifics of this mechanism are detailed later in this chapter.

Winning[7] worked with perhaps one of the most sensitive explosives known - nitroglycerine. The nitroglycerine was poured into a container and an initiator was placed in the centre and fired. Detonation in the nitroglycerine started at the initiator at the centre of the container. With de-gassed nitroglycerine Winning's microsecond framing camera photographs of the event clearly showed an inert shock wave travelling through the nitroglycerine much like it would through water. On

reflection at the container wall, cavitation occurred and detonation started.

King[8] tested the sensitivity of ammonium nitrate at various temperatures. At 170°C he found ammonium nitrate to be a quiescent melt with little decomposition into ammonium gas, NH_3, and nitric acid, HNO_3. The density was 1.4 g/cc at this temperature. This composition could not be detonated with several kilograms of high explosive primer placed right in the melt. The primer generated a pressure of 220 Kbars. As the temperature was increased he found a significant increase in the rate of thermal decomposition resulting in some of the ammonia gas not being vented from the melt. At 260°C the density of the melt was 0.8 g/cc and it could be detonated by an electric blasting cap which contains less than 1 g of high explosive. To prove that this sensitivity increase was due to the voids and not to the temperature or acid level, King added microballoons, hollow gas filled glass spheres, to an inert melt at 170°C to reproduce the same density as at 260°C. He found an increase in ammonium nitrate sensitivity corresponding to the increase for the 260°C temperature condition.

Modeling of the effect of pressure on hot-spots has been attempted by Bruckmann and Guillet.[9] The aspect of the problem which they considered was that of the heat generated at the surface of the hot-spot due to chemical reaction and the loss

of heat due to conductivity away from the reacting surface. In order for the hot-spot to be effective as an initiator then it is necessary for its temperature to exceed a certain critical temperature above which the reaction (decomposition) energy is greater than that dissipated and lost. When this condition is met the temperature will continue to rise until detonation occurs. For several pure monomolecular explosives they calculated the critical temperature for detonation based on a first order decomposition and using heat conduction as the only loss. A first order decomposition was used to calculate the reaction rate and the rate of heat production. From this the temperature in the hot-spot after a given time interval was calculated by an iterative method. Heat loss over this time interval was calculated solving a conduction equation. If there was a net gain in temperature for the time interval chosen this led to detonation. A net loss would lead to failure.

The critical temperatures could be determined as a function of the size of the hot-spot. There appeared to be optimum sizes for a specified time interval.

The activation energies used were those published by other researchers for monomolecular explosives and were determined by isothermal decomposition testing. The critical temperatures correlated quite well with the results of impact (drop weight) tests for these explosives.

A further result of this study showed that the critical temperature increased slowly as the density was decreased. This

was slow at first but increased rapidly until a critical density was reached generally between 0.4 and 0.5 gm/cm^3. They stated that at these densities or lower the heat generated in the hot-spot was never greater than the heat loss due to conduction. Hence the explosive is insensitive to hot-spot initiation under these conditions. This would appear to be a weakness with this model since it is possible to detonate monomolecular explosives such as nitroquanidine frothed down to densities of 0.11 gm/cc.[10]

Other serious weaknesses were the activation energies used. These are determined from isothermal decomposition data determined at relatively low temperatures and pressures. The question which arises is how good are these values under high temperature and pressure conditions. Also there is the question of the decomposition reaction which occurs and which is the rate controlling step and whether this changes under high temperature and pressure conditions. There is considerable evidence that this is indeed often the fact[11]. For this reason theoretical initiation models are of limited applicability.

It is known that the decomposition of an explosive is thermal in origin. Calculations will now be made to determine the bulk temperature rise in an ungassed explosive such as nitromethane when subjected to planar shocks of various intensities. Absolute rates of reaction will be calculated for

these temperature rises and compared to the reaction for gassed nitromethane under the same pressure conditions.

The theory outlined here is essentially the theory presented by Cook[11], Taylor[12] and von Elbe[13]. Consider a planar shock wave travelling through a stationary liquid explosive. The liquid is assumed to be of infinite extent parallel to the plane of the shock wave so that there are no edge effects. The flow is one-dimensional. The wave front advances through the liquid at a transmission speed, D. The original pressure, temperature, density, specific volume, and internal energy per unit mass are P_1, T_1, ρ_1, V_1, and E_1 before the shock wave arrives. In the shock wave these variables change to P_2, T_2, ρ_2, V_2, and E_2. The particle velocity in the shock is W. The mass flow through unit area of the wave in unit time is $\rho_1 D$.

From the law of conservation of mass:

$$\rho_1 D = \rho_2 (D - W) \qquad (2.1)$$

For unit area the mass flow into the front in time dt has momentum $\rho_1 D^2 dt$ and the mass flow out has a momentum $\rho_1 D(D - W)dt$. Conservation of momentum requires that the difference in momentum must equal the impulse or net force per unit area when $dt \to 0$. Thus:

$$\rho_1 D^2 dt - \rho_1 D(D - W)dt = (P_2 - P_1)dt$$

OR

$$P_2 - P_1 = \rho_1 DW \tag{2.2}$$

Conservation of energy requires that the sum of the internal energy, the potential energy, and the kinetic energy is constant. Thus the input in unit time through a unit cross-sectional area will be equal to the output:

$$E_1(D\rho_1) + P_1 D + \tfrac{1}{2}(\rho_1 D)D^2 = E_2(D - W)\rho_2 + P_2(D - W) + \tfrac{1}{2}\rho_2(D - W)(D - W)^2 \tag{2.3}$$

Because of (2.1), (2.3) becomes:

$$E_1 + \frac{P_1}{\rho_1} + \tfrac{1}{2}D^2 = E_2 + \frac{P_2}{\rho_2} + \tfrac{1}{2}(D - W)^2 \tag{2.4}$$

From (2.1):

$$D = \left(\frac{\rho_2}{\rho_2 - \rho_1}\right) W \tag{2.5}$$

From (2.2):

$$W = \frac{P_2 - P_1}{\rho_1 D} \tag{2.6}$$

From (2.5)(2.6):

$$D^2 = \left(\frac{\rho_1}{\rho_2 - \rho_1}\right)\left(\frac{P_2 - P_1}{\rho_1}\right) \tag{2.7}$$

By making substitutions $V_2 = 1/\rho_2$, $V_1 = 1/\rho_1$; (2.7) yields:

$$D = V_1 \left(\frac{P_2 - P_1}{V_1 - V_2}\right)^{\frac{1}{2}} \tag{2.8}$$

Similarly from (2.5):

$$W = (V_1 - V_2) \left(\frac{P_2 - P_1}{V_1 - V_2}\right)^{\frac{1}{2}} \tag{2.9}$$

(2.4) yields:

$$E_1 - E_2 = \frac{P_2}{\rho_2} - \frac{P_1}{\rho_1} + \tfrac{1}{2}(D - W)^2 - \tfrac{1}{2}D^2 \tag{2.10}$$

Substitute (2.8) and (2.9) into (2.10) to yield:

$$E_1 - E_2 = \tfrac{1}{2}(P_2 + P_1)\ (V_2 - V_1) \qquad (2.11)$$

OR

$$E_2 - E_1 = \tfrac{1}{2}(P_2 + P_1)\ (V_1 - V_2) \qquad (2.12)$$

From (2.1):

$$W = D\left(1 - \frac{\rho_1}{\rho_2}\right) \qquad (2.13)$$

From (2.2) and (2.13):

$$P_2 - P_1 = \rho_1 D^2\ [1 - \rho_1/\rho_2] \qquad (2.14)$$

Substituting $V_2 = 1/\rho_2$, $V_1 = 1/\rho_1$ into (2.13)

$$\frac{W}{D} = (1 - V_2/V_1) \qquad (2.15)$$

Since $P_2 \gg P_1$ then (2.2) becomes:

$$P_2 = \rho_1 DW \qquad (2.16)$$

(2.14) becomes:

$$P_2 = \rho_1 D^2[1 - \rho_1/\rho_2] \qquad (2.17)$$

and (2.12) becomes:

$$E_2 - E_1 = \tfrac{1}{2}P_2(V_1 - V_2) \qquad (2.18)$$

which is called the RANKINE-HUGONIOT EQUATION.

Also: $E_2 - E_1 = C\,(T_2 - T_1)$ (2.19)

where C is the specific heat of the liquid explosive.

Experimentally, a relationship can be determined for the shock velocity versus particle velocity. The Los Alamos Group[6] has determined this relationship for nitromethane to be:

$$D = 1647 + 1.637\ W \qquad (2.20)$$

where: D = shock velocity (m/s)

W = particle velocity (m/s)

For nitromethane: ρ_1 = 1.14 g/cc OR V_1 = 0.88 cc/g

From the experimental relationship (2.20):

$$W/D = 0.61 - \frac{1006}{D}$$

From equation (2.15):

$$W/D = (1 - V_2/V_1)$$

therefore: $W/D = (1 - V_2/0.88) = (0.61 - 1006/D)$

For any value of shock velocity, D, W/D can be calculated, so can V_2 from equation (2.15) and P_2 from equation (2.16). From V_2, $(V_2 - V_1)$, can be calculated and knowing the specific heat of nitromethane, 0.412 cal/g/°C, ΔT can be calculated using equation (2.19).

Table 1 contains values for ΔT and T_{2n}, for various shock velocities and pressures imparted to nitromethane, assuming T_1 = 288°K. T_{2n} is the temperature to which the non-gassed

nitromethane is bulk heated. Values of W/D, W, P_2, V_2 and $V_1 - V_2$ are also tabulated. Appendix A contains a sample calculation.

If voids exist in a solid, or if gas bubbles are entrapped in a liquid, then upon being shocked these voids or bubbles undergo adiabatic compression to a high temperature. For an ideal gas the temperature reached inside a compressed bubble, T_2 degrees absolute, depends on the compression ratio and is given by:

$$T_2 = T_1\left(\frac{P_2}{P_1}\right)^{[(\gamma - 1)/\gamma]} \qquad (2.21)$$

where: P_1 = initial pressure inside the bubble, atm

T_1 = initial temperature inside the bubble, °K(288°K)

P_2 = final pressure inside the bubble, atm

T_2 = final temperature inside the bubble, °K

γ = ratio of specific heats, 1.4 for air.

P_1 is atmospheric pressure = 1 atm or .0010 Kbars. P_2 is the pressure generated by the shock as it is for the non-gassed nitromethane case.

D (m/s)	W/D	W (m/s)	P_2 (Kbars)	V_2 (cc/g)	$V_1 - V_2$ (cc/g)	$E_1 - E_2$ (cal/g)	ΔT (°K)	T_{2n} (°K)
3000	0.2747	824	28.17	0.638	0.242	81.28	197.27	485.27
3500	0.3226	1129	45.03	0.596	0.284	152.47	370.07	658.07
3600	0.3306	1190	48.82	0.589	0.291	169.38	411.11	699.12
3700	0.3381	1251	52.75	0.582	0.298	187.41	454.88	742.88
3800	0.3453	1312	56.81	0.576	0.304	205.90	499.78	787.78
3900	0.3521	1373	61.02	0.570	0.310	225.52	547.39	835.39
4000	0.3585	1434	65.36	0.559	0.315	245.46	595.78	883.78
4100	0.3646	1495	69.85	0.554	0.321	267.32	648.84	936.84
4200	0.3705	1556	74.47	0.549	0.326	289.44	702.53	990.53
4300	0.3760	1617	79.23	0.544	0.331	312.66	758.89	1046.89
4400	0.3814	1678	84.13	0.540	0.336	337.02	818.00	1106.00
4500	0.3864	1739	89.18	0.536	0.340	361.50	877.42	1165.42

TABLE 1: RESULTS OF CALCULATION OF T_{2n}, FINAL TEMPERATURE OF NON-GASSED NITROMETHANE, FOR VARIOUS SHOCK VELOCITIES.

Table 2 contains values for T_{2g} for the various pressures imparted to the gassed nitromethane and T_{2n} for the same pressures imparted to the non-gassed nitromethane calculated earlier. Appendix B contains a sample calculation for T_{2g}. The temperature increase when shocked is much greater at the gas inclusions than in the liquid itself. As such it is evident that initiation will begin at these hot-spots and that these entrapped air bubbles have a great effect on the sensitivity of an explosive.

Chemical reaction rates vary exponentially with temperature according to the Eyring rate equation:

$$kr = \frac{kT}{h} \; e^{(-\Delta F^*/RT)} \qquad (2.22)$$

where kr = absolute reaction rate, sec^{-1}.

k = Boltzmann's constant, 3.30×10^{-24} cal/°K

h = Planck's constant, 1.58×10^{-34} cal·s

R = the gas constant, 1.987 cal/mol/°K

ΔF^* = activation energy, cal/mol

T = temperature, °K

P_2 (Kbars)	NON-GASSED T_{2n} (°K)	GASSED T_{2g} (°K)	k_{2g}/k_{2n}
28.17	485.27	5600	3.35×10^{11}
45.03	658.07	6420	3.72×10^{8}
48.82	699.12	6570	1.20×10^{8}
52.75	742.88	6720	4.09×10^{7}
56.81	787.78	6860	1.53×10^{7}
61.02	835.39	7010	6.10×10^{6}
65.36	883.78	7150	2.63×10^{6}
69.85	936.84	7290	1.15×10^{6}
74.47	990.53	7420	5.46×10^{5}
79.23	1046.89	7560	2.71×10^{5}
84.13	1106.00	7690	1.40×10^{5}
89.18	1165.42	7820	7.69×10^{4}

TABLE 2: COMPARISON OF FINAL TEMPERATURES AND RATIO OF ABSOLUTE REACTION RATES FOR GASSED AND NON-GASSED NITROMETHANE.

Consider the absolute reaction rate equations for non-gassed nitromethane and gassed nitromethane at a shock pressure of 84.13 Kbars. For the non-gassed nitromethane:

$$k_{2n} = \frac{kT_{2n}}{h} \; e^{(-\Delta F^*/RT_{2n})}$$

For the gassed nitromethane:

$$k_{2g} = \frac{kT_{2g}}{h} \; e^{(-\Delta F^*/RT_{2g})}$$

Then the ratio of the absolute reaction rates:

$$\frac{k_{2g}}{k_{2n}} = \frac{T_{2g}}{T_{2n}} \times \frac{e^{(-\Delta F^*/RT_{2g})}}{e^{(-\Delta F^*/RT_{2n})}} \qquad (2.23)$$

$$\frac{k_{2g}}{k_{2n}} = \frac{T_{2g}}{T_{2n}} \; e^{\left[\frac{-\Delta F^*}{R}\left(\frac{1}{T_{2g}} - \frac{1}{T_{2n}}\right)\right]}$$

OR

$$\frac{k_{2g}}{k_{2n}} = \frac{T_{2g}}{T_{2n}} \; e^{\frac{\Delta F^*}{R}\left[\left(\frac{1}{T_{2n}} - \frac{1}{T_{2g}}\right)\right]} \qquad (2.24)$$

At a pressure of 84.13 Kbars the calculated values of T_{2g} = 7690°K, T_{2n} = 1106°K are in Table 2. For nitromethane ΔF^* ≈ 25600 cal/mole [11] and since R = 1.987 ≈ 2 cal/mole/°K then equation (2.24) becomes:

$$\frac{k_{2g}}{k_{2n}} = \frac{7690}{1106} \; e^{\left[\frac{25600}{2}\left(\frac{1}{1106} - \frac{1}{7690}\right)\right]}$$

and $k_{2g}/k_{2n} = 1.40 \times 10^5$

Since the reaction rate is proportional to the absolute reaction rate constant the inclusion of gas bubbles increase the reaction rate of nitromethane by a factor of approximately 1.40 x 10^5 under a shock pressure of 83.07 Kbars.

Table 2 contains similar reaction rate factors calculated for the pressures and temperature rises calculated earlier.

Two products tested in this report rely on air bubble sensitization for initiation through adiabatic bubble compression. The AN/FO relies on compression of its voids also.

Hot reaction products from the donor charge in this compressional shock wave can also help provide directly the necessary enthalpy for detonation in the receptor charge. Of course these hot products would have little or no effect across inert condensed gap media, such as sand[11]

2.1.2 Initiation in Explosives Sensitized with Hollow Glass Microbubbles

Air bubble sensitized explosives can undergo desensitization at the bottom of deep boreholes. This is due to the air voids becoming precompressed by hydrostatic head and thereby becoming less effective as hot-spot reaction centers when the primers in the explosive are detonated.

To avoid precompression and void migration, some explosives are sensitized by rigid hollow microbubbles containing air at slightly negative pressure. The usual size of microbubbles is about 60 - 70μ with a size distribution between 40 and 100μ. The compressive strength of the microbubbles varies from approximately 150 atm to 700 atm.

Providing the shock from the primer or donor charge, is large enough, the glass microbubbles in the receptor charge will collapse in the shock. Two schools of thought prevail which explain the degradation of this mechanical energy, to heat energy. The first view[12] is that upon microbubble collapse the air inside the microbubble becomes adiabatically compressed to a

high pressure and hence a high temperature increase occurs. This is similar to the case of the initiation of air bubble sensitized products discussed earlier.

An alternate view[14] is that the microbubbles are collapsed by the compressive shock from the donor charge and form high velocity silica microjets. It is thought that friction from these microjets raises the temperature of the surrounding liquid explosive thereby causing deflagration and eventually detonation. This mechanism would be similar to a bulk decomposition mechanism. To form high velocity microjets quite intense shock pressures would be required.

Detailed discussion on the validity of these two views is beyond the scope of this report and subsequent experimental results for those products believed to contain microbubbles are discussed using both theories.

2.2 PARAMETERS AFFECTING DETONATION

This section briefly outlines the effect of charge diameter, degree of confinement, temperature and pressure on the detonation characteristics of air bubble and microbubble sensitized explosives. The Detonation Head Model after Cook[11] will be used to illustrate the effects of these parameters.

2.2.1 Detonation Head Model

The detonation of an explosive can be either ideal or non-ideal. Ideal detonation corresponds to the complete reaction of explosive inside the detonation wave. Non-ideal corresponds to incomplete reaction.

Cook[11] states: "non-ideal detonation refers to steady state wave propagation at a velocity lower than ideal. It is related to the rate of conversion of the explosive to its products of detonation and lateral heat or pressures losses."

In cylindrical charges between the critical diameter, the diameter below which a steady detonation does not occur, and the minimum diameter at which ideal detonation is observed, it can be noted that the velocity of detonation increases with charge diameter. Although these detonations are non-ideal they may be stable at that particular charge diameter.

Figure 4 indicates what happens when a detonation wave travels in an air or gas bubble sensitized explosive charge confined in a borehole. The detonation front, and side expansion waves define a region called the detonation head. The air pockets in the explosive are compressed adiabatically in the shock front and act as reaction centres throughout the detonation head. Energy released in the detonation head goes to supporting the detonation. Figure 5 shows the same process in an explosive

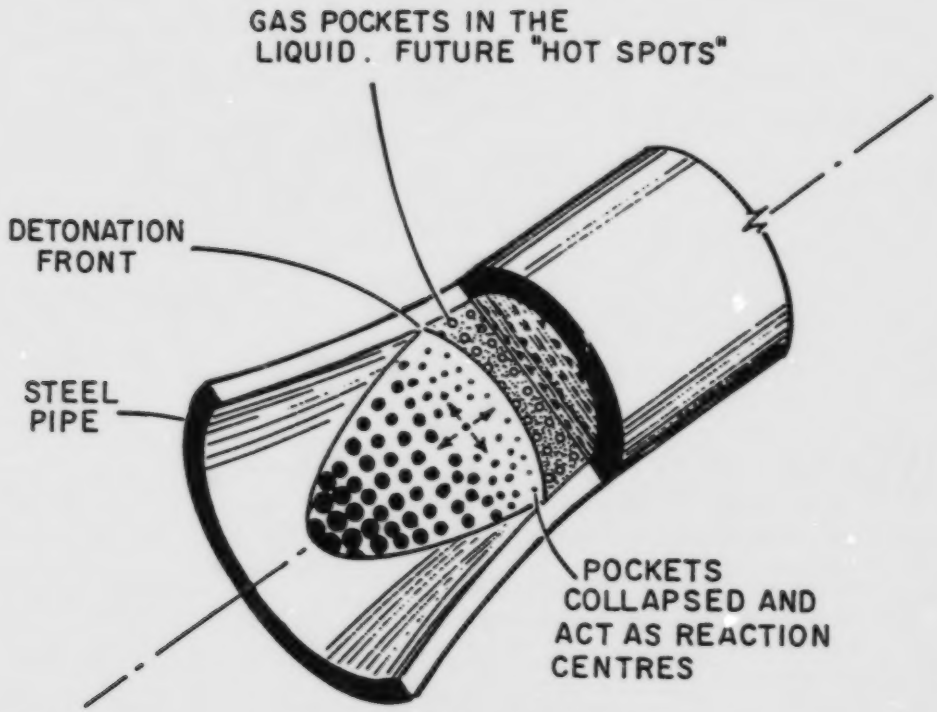

FIGURE 4 : DETONATION PROCESS IN A CYLINDRICAL LIQUID EXPLOSIVE SENSITIZED BY ENTRAPPED AIR BUBBLES. (15)

sensitized with hollow glass microbubbles. The hot-spots may be formed by adiabatic collapse or microjet formation.

The shape of the detonation head depends on the geometry of the charge. The length of the head depends on the diameter of the charge and whether it is confined or not. The length of the detonation head in an unconfined charge is approximately equal to the diameter of the charge. The length when confined is approximately 1 1/3 times as long as the charge diameter. Experimental results[11] indicate that the length is independent of charge density and charge composition. The conical shape shown in Figures 4 and 5 is formed at a distance of about 3 1/2 - 5 1/2 times the charge diameter down the charge from the primer, depending on confinement.

As the explosive enters the detonation head it reacts. Energy is liberated by this reaction and goes towards sustaining the detonation. If the time needed for the fluid explosive to fully react is longer than the time it is allowed to react as it passes through the detonation head, the energy liberated is not the total energy possible and the detonation velocity and pressure output will be less than the theoretical maximum. As the charge diameter is increased the length of the detonation head increases and at some detonation head length, or charge diameter, all of the explosive has time to react fully and the theoretical detonation velocity, and pressure output, is achieved. At charge diameters greater than this, detonation

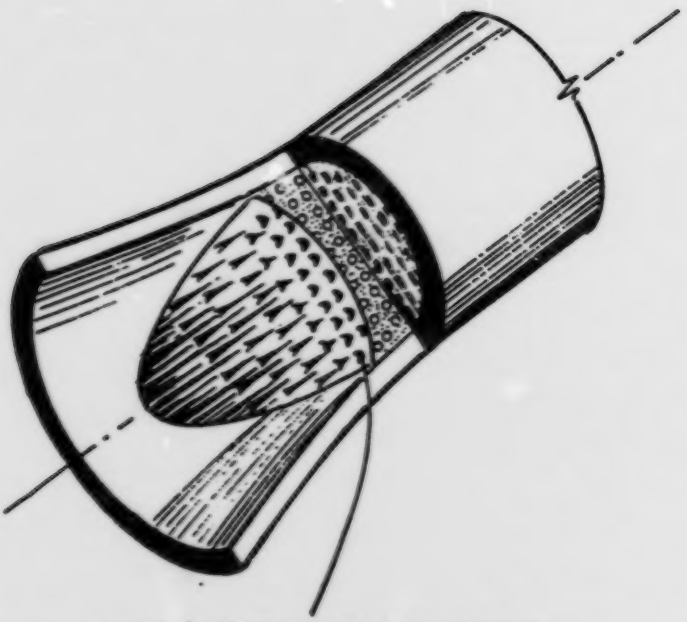

GLASS MICROBUBBLES BEING COLLAPSED TO FORM HIGH VELOCITY JETS ACTING AS REACTION CENTRES.

FIGURE 5 : DETONATION PROCESS IN A CYLINDRICAL LIQUID EXPLOSIVE SENSITIZED BY GLASS MICROBUBBLES. (15)

velocity does not increase, pressure output does not increase, but the length of the detonation head increases thereby increasing the impulse or duration of the pressure.

Therefore in addition to the normal scaling up of gap distance with charge diameter, the effect will be enhanced by the increase in peak pressure and duration. In fact the peak pressure from the donor charge will be increased by a factor of approximately $(D_1/D_2)^2$ due to an increase in charge diameter.[15]

2.2.2 Influence of Confinement

The effect of confinement is to lower the rate of expansion of the gasses off the side of the charge thereby extending the length of the detonation head.

This increase in the length of the detonation head allows more time for the fluid explosive to react. Therefore more energy will be available for sustaining the detonation and the velocity of detonation will increase, as will the peak pressure. With an increase in the length of the detonation head the impulse will also increase.

Confinement has a pronounced effect on the impulse and the detonation velocity and hence the shock velocity of the donor charge. It is apparent that if gap sensitivity research results are to be applied to mining situations, confinement of the charges is a requirement.

2.2.3 Influence of Temperature Reduction on Explosive Sensitivity

The effect of reduced temperature is to reduce the explosive sensitivity to initiation by a primer normally used at warmer temperatures. However in the case of microbubble sensitized explosives the increase in critical diameter and decrease in sensitivity with reduced temperature is negligible providing no crystallization occurs. One is referred to the study of temperature effects on emulsion and slurry by P. Katsabanis[16].

In gas bubble sensitized explosives there is a marked reduction in sensitivity and increase in critical diameter as the explosive composition temperature is reduced. The sensitivity reduction is probably due to the shrinkage of the product at the colder temperature and this shrinkage causes precompression of the gap pockets in the product as the gas phase takes up the shrinkage.

If recrystallization or freezing occurs due to a temperature drop the crystals can reduce the sensitivity of fluid explosives, acting as a barrier to transmission of the shock wave. This is because liquids transfer energy more efficiently than solids. While there is some shock intensification due to the reflection from the crystals, the effect of this is less than the sensitivity loss due to the gas pocket loss or shrinkage.

At the present time there is not a fully proven explanation of the behaviour of explosives under low temperatures but the basic models mentioned here are generally accepted as being representative of the phenomena.

2.2.4 Influence of Static Pressures on Explosive Sensitivity

Static overpressures of approximately 50 psi or 3.4 atmospheres can be found at the bottom of 20 m deep charged and stemmed boreholes. If the hole is loaded with an explosive sensitized with microbubbles, providing the hydrostatic head is insufficient to rupture these microbubbles, which is the case, then there is no effect of the hydrostatic head on the product sensitivity.

Entrapped air bubbles which act as hot-spot reaction centres have their effectiveness substantially reduced when they are precompressed under such a static pressure. Thus air bubble sensitized explosives would have their sensitivity reduced and may become "dead-packed" with inadequate sensitivity to sustain the detonation process.

The following is an exercise to illustrate the effect of this static pressure on the sensitivity of a gas bubble sensitized product.

Consider an air bubble sensitized explosive under no hydrostatic head. The air pressure in the bubble is $P_1 = 1$ atm,

the initial temperature in the bubble is T_1 = 288°K and the pressure, P_2, generated by a primer in the explosive is 100,000 atmospheres. Using equation (2.21), detailed earlier, the final temperature reached by the air bubble upon shock by the primer can be calculated as being 8117°K.

Now consider a static overpressure of 50 psi at the bottom of a borehole. The new initial pressure, P_1, in the air bubble is 64.7 psi or 4.4 atmospheres. The bubble is now somewhat precompressed with any heat generated being dissipated to the surroundings. When the primer is fired the bubble is compressed to P_2 = 100,000 atm. The final temperature of the bubble in this case can be calculated as being 5281°K.

The absolute reaction rate in the non-static pressure case is 5.4 times as great as in the static pressure case. This was determined using equation (2.25) detailed earlier since the energy change at absolute zero for a typical ammonium nitrate based explosive is approximately 38,000 cal/mol.

The hot-spots in the pre-compressed product do not reach as high a temperature as the hot-spots in the product at atmospheric pressure. This shows up as a decrease in sensitivity, and increase in critical diameter for this type of explosive under static pressure.

2.2.5 Influence of Dynamic Pressures on Explosive Sensitivity

Explosive products sensitized by entrapped air are influenced by dynamic pressures as are those products sensitized by glass microbubbles.

In some blasting situations explosive cord containing from 5.3 to 12 grams of high explosive per metre length are used to initiate primers at the bottom of holes. As such, these downlines must run the length of the hole in or next to the primary blasting charge. On detonation these downlines can affect the sensitivity of the explosive in the borehole. For example if the explosive is sensitized with microbubbles the pressure wave from the downline when it detonates can rupture these glass spheres. Once ruptured and collapsed it is not possible for the hot-spot jet action to occur and the explosive becomes desensitized. Alternately with the adiabatic compressed air model the air void size is reduced to a level where it is less effective due to the smaller reactive surface.

In explosives that are sensitized with entrapped air bubbles the shock from the detonating downline collapses the bubbles as it passes by. As the pressure from the detonating downline decreases these bubbles relax back to their normal state before the primer is detonated.

Dynamic pressure effects can also desensitize microbubble sensitized products when blastholes are too close

together. For example, such products can be used in small diameter holes underground in drift blasting. If the blastholes are completely filled with explosive and are too close together failures can occur in holes fired on later delay periods if the stress wave from holes fired on previous delays is strong enough to rupture the microbubbles. With 45 mm diameter holes failures can occur up to 45 cm away due to this dynamic pressure desensitization[15]. Once again, air bubble sensitized systems do not suffer from this problem.

One solution to the above problem is to use charges of smaller diameter than the hole diameter, decouple the charges, so that the stress wave intensity into the charge is reduced. However before reaching for such a solution it needs to be evaluated in the laboratory in order to ensure that failures do not now occur due to the so-called "channel-effect". This is the effect which takes placed when decoupled charges are fired in boreholes. The effect is caused by the gaseous products of detonation. They expand out into the vacant space surrounding the charge but their expansion is limited and their velocity down the annular space increases due to the piston effect. As the detonation travels down the charge the gases travel down the annular space. If the explosive has a relatively low velocity of detonation, which would be true in many cases in smaller charge diameter applications, then it is possible for the gases to outrun the detonation. When this occurs pressure is applied to

the explosive ahead of the detonation wave. In some cases failures result due to this precompression. At the present time the phenomena referred to has been observed on a number of occasions but it has not been quantified in terms of the extent of the decoupling versus velocity of detonation etc.

2.2.6 Influence of the Gap Material Type on the Propagation of Detonation Across a Gap

As detailed earlier, a confined donor explosive charge upon detonation produces a shock wave directed towards the receptor charge. This shock wave may contain or may be closely followed by the hot products of the donor decomposition, also directed towards the receptor charge. The type of inert medium between the donor and receptor charges may have a pronounced effect on the ability of the donor charge to initiate receptor charge detonation at a given gap distance.

If the gap is composed of water or sand the projection of hot products from the donor charge detonation will have little effect on the receptor charge. Propagation in these cases relies on the shock from the donor traveling through the media to the receptor charge.

If the amount of shock pressure impacting the receptor charge is the only criterion for its initiation, one would expect larger water gap distances cross-propagated and longer sand gap distances cross-propagated than those cross-propagated for an air

gap. Water and sand transmit pressure more efficiently than air.[11] However if the effect of the hot products from the donor charge are also considered, their loss may offset the increase in pressure impacting the receptor charge in these media and the net gap distance cross-propagated may decrease when water is substituted for air.

The difficulties with modelling gap sensitivity testing are many and are associated with all aspects of the problem: the donor detonation properties, the receptor initiation, and the transfer of detonation through the gap material.

Donor charge peak pressure, pressure duration or impulse, and shock velocity are all affected by the composition of the explosive, the charge diameter, the degree of confinement, the temperature, etc. This is one group of variables that makes modelling of gap sensitivity testing difficult.

In addition there is the mode of receptor charge sensitization by hot-spots. The fact that the explosives in use are heterogeneous causes difficulty in modeling a burning or reaction process which requires input data such as activation energy for the rate determining step. Even in pure monomolecular explosive systems there is extreme difficulty. For example, the majority of activation energies that are in the published literature have been determined from weight loss experiments conducted at relatively low temperatures, compared to the

temperatures reached in the decomposition process, and at relatively low pressures (several atmospheres). Cook[11] gives examples when activation energy values change at high temperature.

There are also problems of modelling and determining actual bubble distributions and burn distances.

Modeling gap materials such as sand would pose a problem. If the gap material was a pure solid it could be modeled with a finite element approach but the composite nature of sand makes it difficult.

In pure monomolecular explosive systems the problems mentioned exist. Commercial explosive systems, of concern here, are very much more complex. The degree of difficulty in modeling the gap phenomena is enhanced due to a wide variety of product ingredients and phases: solid, liquid and gas.

Because of the foregoing reasons, initiation and detonation theory are used to explain the experimental data presented in this report in a qualitative manner only, but none the less they do give insight into the cross-propagation process.

CHAPTER 3

EXPERIMENTAL DESIGN AND INSTRUMENTATION

3.0 INTRODUCTION

Experimental investigations often deal with continuous variables which cannot be measured in practice. In this case, the testing of the sensitivity of an insitu explosive to shock from a donor charge at various sand gap distances is of concern. There are distances at which some receptors will detonate and others will not, and it is assumed that those which do not detonate would have detonated if the distance between donor and receptor was shortened sufficiently. It is supposed, therefore, that there is a critical distance associated with each explosive product and that the product should detonate when the donor charge is closer than that distance. It is also supposed that the product should not detonate when the donor charge is further away than that distance.

The population is thus characterized by this variable - the P50 gap distance - which cannot be measured. All that can be done is to select some distance arbitrarily and determine whether the P50 gap distance for a given product at a given charge diameter is less than or greater than the selected gap distance.

There are several well known statistical methods for determining this P50 gap distance. Two methods are described here. Both have their merits.

3.1 THE GRAPHICAL SOLUTION

In sensitivity experiments it is not possible to make more than one observation on a given specimen. If the test fails - the receptor charge is altered by the donor detonation. If the test result is positive - the receptor charge detonates. A common procedure in experiments of this kind is to divide the sample of specimens into several groups (not necessarily of the same size) and to test one group at a chosen gap distance, a second group at a second gap distance, and so on. The resulting data then consist of the number of receptor charges detonating at each gap distance. A graphical analysis of the data may then be made.

Table 3[4] contains hypothetical data for an illustration of this graphical method. Twenty specimens are tested at each of seven gap distances with the number of receptor charge detonations given for each gap distance. These data are plotted as a log-normal-probability graph in Figure 6[4], and the best fit line was drawn (by eye in this case).

From this line the median is estimated to be P50 = 38 cm, and the values P95 = 5 cm and P05 = 300 cm can be easily

GAP DISTANCE (cm)	NUMBER OF TESTS	NUMBER OF RECEPTOR DETONATIONS	PROBABILITY OF RECEPTOR DETONATION (%)
5	20	19	95
10	20	17	85
20	20	15	75
40	20	9	45
80	20	6	30
160	20	2	10
320	20	0	0

TABLE 3: HYPOTHETICAL DATA FOR AN ILLUSTRATION OF THE GRAPHICAL METHOD[4].

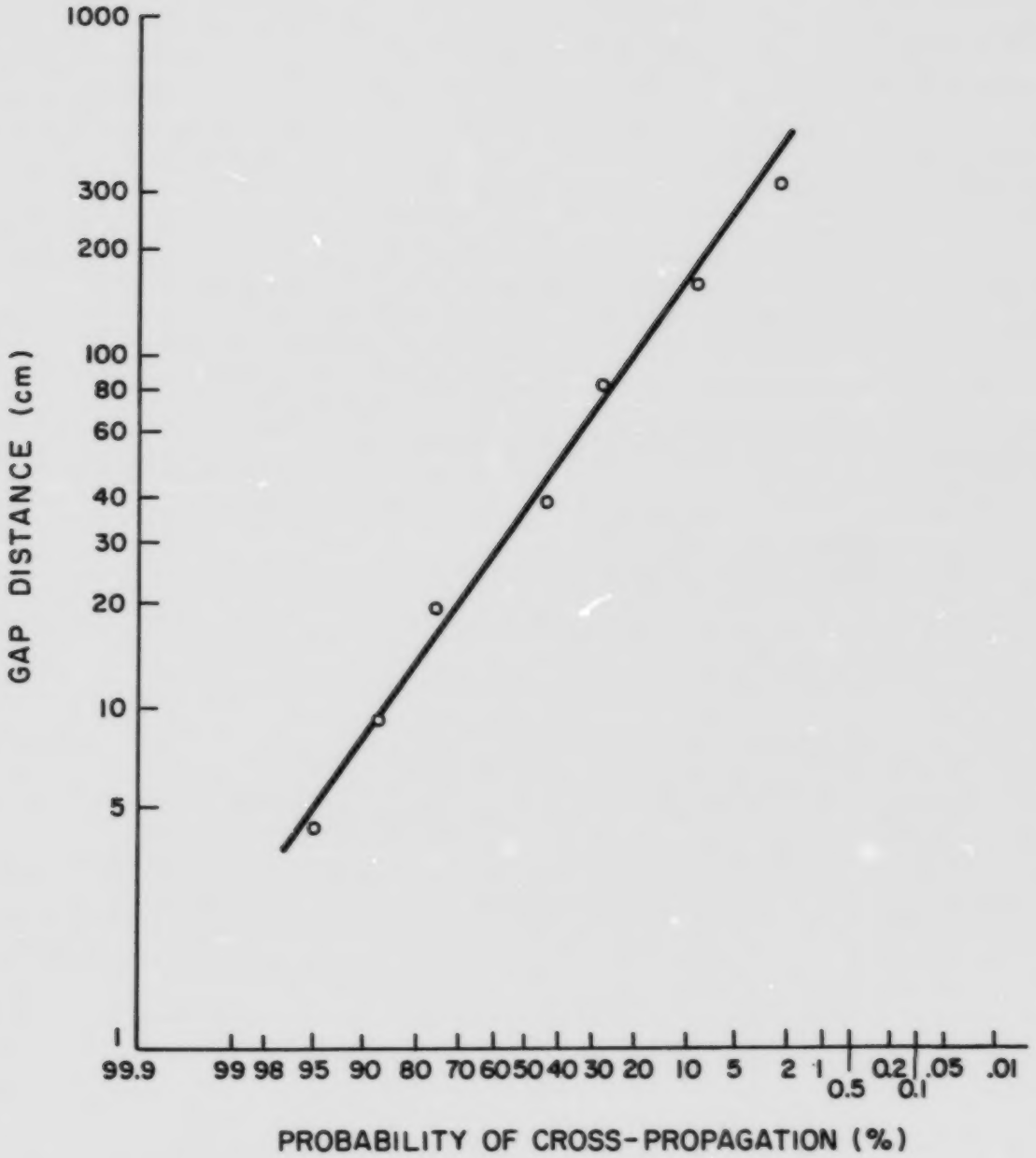

FIGURE 6 : GRAPHICAL REPRESENTATION OF SAMPLE DATA (4).

found. The P95 point is the gap distance at which the probability of cross-propagation is 95%. The P05 point is the gap distance at which the probability of cross-propagation is 5%. In this case it is not possible to determine the gap distances at 0 and 100 percent probability of propagation as the logarithm of the original data is normally distributed.[4] The P95 and P05 gap distances are important explosive characteristics in that mine operators are concerned with blasting methods that require either absolute cross-propagation or absolutely no cross-propagation.

Ideally, for the sake of utmost accuracy, one would prefer to use this method for testing all of the explosive types at all charge diameters considered by this research. However, this would necessitate thousands of tests and would make this research economically unfeasible.

With this in mind, an alternate method widely used in go/no-go experimental research was adopted. This method, described below, is valuable in determining the P50 gap distances for explosive products. The results are also used to estimate the P95 and P05 gap distances.

3.2 THE "UP-AND-DOWN" METHOD

The "Up-and-Down" method[2,3,4] is a technique for obtaining explosive sensitivity data. The primary advantage of

this method is that it concentrates testing near the mean and allows the P50 gap distance to be determined with relatively few tests.

The technique is to choose some initial gap distance Xo and perform the first test at this distance. If the receptor charge detonates, the second specimen will be tested at Xo + d, where d is the gap distance interval. If the receptor charge fails then the second specimen will be tested at Xo - d. The value of d should be chosen to equal the standard deviation, σ, of the distribution of the gap distances around the mean gap distance. However, as mentioned later, the error increase in the determination of the P50 gap distance when $d \neq \sigma$ is not significant[4]. The value of d was chosen as 3, 6, or 12 inches, 7.5, 15.2, 30.5 cm in this research depending on the charge diameter. At larger charge diameters larger gap distances are cross-propagated, and a larger value of d is used, 12 inches (30.5 cm).

In general, any specimen will be tested at a gap distance immediately longer or immediately shorter than the gap distance of the previous test, according to whether there was or was not a receptor charge detonation on the previous test.

An appropriate way to describe this technique is to list the steps in the procedure and then calculate actual P50 values for two examples:

A) An initial gap distance is chosen, Xo, as near as

possible to the anticipated P50 gap distance.

B) A series of tests is carried out following the rule of an increase in gap distance, X_o+d, following a receptor charge detonation and a decrease in gap distance, X_o-d, following a receptor charge failure.

C) The number N^1 is the total number of gap tests performed for a given charge and diameter. Testing continues until a "nominal" sample size = N is reached. N is the total number of trials, N^1, reduced by one less than the number of like responses at the beginning of the series. For example, if the results were 2 cross-propagations then a failure then another cross-propagation and failure, the results would be: YYNYN at various gap distances. N^1 in this case is 5 tests. N is 5 -(2 - 1) = 4 tests since there are 2 like responses at the beginning of the test series.

D) For N≤6, the resulting configuration of cross-propagations and receptor charge failures for each series is in Table 4 which has been reproduced from a publication by Dixon and Massey[4]. This table contains correction factors k, calculated by Dixon and Massey for typical Y-N response configurations. Dixon solves for the mean gap distance, μ or P50:

VALUES OF k FOR DETERMINING P50 FROM UP-AND-DOWN SEQUENCE OF TRIALS OF NOMINAL LENGTH N. THE ESTIMATE OF P50 IS x_1 + kd WHERE x_1 IS THE FINAL GAP DISTANCE AND d IS THE INTERVAL BETWEEN GAP DISTANCES. IF THE TABLE IS ENTERED FROM THE FOOT, THE SIGN OF k IS TO BE REVERSED.

N	SECOND PART OF SERIES	k FOR TEST SERIES WHOSE FIRST PART IS Y	YY	YYY	YYYY	
2	N	-.500	-.388	-.378	-.377	Y
3	NY	.842	.890	.894	.894	YN
	NN	-.178	.000	.026	.028	YY
4	NYY	.299	.314	.315	.315	YNN
	NYN	-.500	-.439	-.432	-.432	YNY
	NNY	1.000	1.122	1.139	1.140	YYN
	NNN	.194	.449	.500	.506	YYY
5	NYYY	-.157	-.154	-.154	-.154	YNNN
	NYYN	-.878	-.861	-.860	-.860	YNNY
	NYNY	.701	.737	.741	.741	YNYN
	NYNN	.084	.169	.181	.182	YNYY
	NNYY	.305	.372	.380	.381	YYNN
	NNYN	-.305	-.169	-.144	-.142	YYNY
	NNNY	1.288	1.500	1.544	1.549	YYYN
	NNNN	.555	.897	.985	1.000	YYYY
6	NYYYY	-.547	-.547	-.547	-.547	YNNNN
	NYYYN	-1.250	-1.247	-1.246	-1.246	YNNNY
	NYYNY	.372	.380	.381	.381	YNNYN
	NYYNN	-.169	-.144	-.143	-.142	YNNYY
	NYNYY	.022	.039	.040	.040	YNYNN
	NYNYN	-.500	-.458	-.453	-.453	YNYNY
	NYNNY	1.169	1.237	1.247	1.248	YNYYN
	NYNNN	.611	.732	.756	.758	YNYYY
	NNYYY	-.296	-.266	-.263	-.263	YYNNN
	NNYYN	-.831	-.763	-.753	-.752	YYNNY
	NNYNY	.831	.935	.952	.954	YYNYN
	NNYNN	.296	.463	.500	.504	YYNYY
	NNNYY	.500	.648	.678	.681	YYYNN
	NNNYN	-.043	.187	.244	.252	YYYNY
	NNNNY	1.603	1.917	2.000	2.014	YYYYN
	NNNNN	.893	1.329	1.465	1.496	YYYYY

	N	NN	NNN	NNNN	SECOND
	-k FOR SERIES WHOSE FIRST PART IS				PART OF SERIES

TABLE 4: TABLE USED IN THE CALCULATION OF THE P50 GAP DISTANCE FOR N LESS THAN OR EQUAL TO SIX[4].

$$P50 = X_f + kd \qquad (3.1)$$

where Xf is the last gap distance tested, k is the tabular value and d is the gap distance interval. Fortunately, estimates for the value of P50 prove to have standard errors which depend very little on the actual value of σ and, in addition, are almost independent of the starting level and the mean, P50. This is true even when d differs from σ.[4]

E) For N>6, P50 may be estimated by computing for the last N trials the mean of the test levels corrected by a factor which is dependent on the published constants A and C of Table 5.[4] The value of C is a pre-calculated correction factor which depends on the number of like responses at the beginning of the trials. The value of A is also a pre-calculated correction factor which depends on the difference between the number of receptor detonations and failures in the series of tests. The values of A and C are calculated in a similar manner to the value of k in Table 1. For the P50 one computes:

$$P50 = \frac{\Sigma xi}{N} + \frac{d}{N}(A + C) \qquad (3.2)$$

where xi are the test levels and A and C are obtained from the table. The use of these A and C factors is

VALUES OF A AND C FOR DETERMINING P50 FOR N > 6 THE ESTIMATE IS $\Sigma X_i/N + d(A + C)/N$ WHERE X_i ARE THE GAP DISTANCES OF THE FINAL N TRIALS WITH n_N RECEPTOR FAILURES AND n_Y RECEPTOR DETONATIONS AND d IS THE INTERVAL BETWEEN GAP DISTANCES. C = 0 FOR A SERIES WHOSE FIRST PART IS Y.

$n_Y - n_N$	A	C FOR TEST SERIES WHOSE FIRST PART IS			
		YY	YYY	YYYY	YYYYY
5	10.8	0	0	0	0
4	7.72	0	0	0	0
3	5.22	.03	.03	.03	.03
2	3.20	.10	.10	.10	.10
1	1.53	.16	.17	.17	.17
0	0	.44	.48	.48	.48
-1	-1.55	.55	.65	.65	.65
-2	-3.30	1.14	1.36	1.38	1.38
-3	-5.22	1.77	2.16	2.22	3.56
-4	-7.55	2.48	3.36	3.52	3.56
-5	-10.3	3.5	4.8	5.2	5.3
		NN	NNN	NNNN	NNNNN
$n_N - n_Y$	-A	-C FOR TEST SERIES WHOSE FIRST PART IS			

TABLE 5: TABLE USED IN THE CALCULATION OF THE p50 GAP DISTANCE FOR N GREATER THAN SIX.[4]

illustrated in section 3.2.2. In Table 5, N_Y refers to the number of cross-propagations and N_N refers to the number of receptor charge failures in the final N trials.

3.2.1 "Up-and-Down" - Example 1:

This example is taken from the actual test results reported in Chapter 4. It is the result of sand gap tests on the 90 mm diameter Product A.

The resulting up-and-down curve for tests 10 through 39 is:

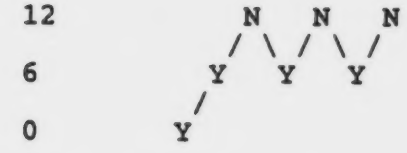

The first test was taken at a gap distance of 0 inches (all field gap test work is reported in inches and the P50 results are converted to centimeters). In this test the receptor charge detonated and the second test was performed at 6 inches (15.2 cm) and the receptor charge detonated. The third test was performed at 12 inches (30.5 cm) and the receptor charge failed, etc...

To calculate the P50 gap distance:

N^1 = 7 total tests

N = 7 - (2 alike initial tests - 1) = 6 nominal

tests (≤6)

Xf = 12 inches, is the final test distance

d = 6 inches, difference between consecutive test levels.

From Table 4[(4)] k can be found to be -.458 and therefore from equation 3.1:

P50 = Xf + kd

= 12 + (-.458)(6)

= 9.3 in. (24 cm)

3.2.2 "Up-and-Down" - Example 2

This example is also taken from the actual test results reported in Chapter 4. It is the result of the sand gap tests on the 150 mm diameter Product B.

The resulting up-and-down curve for tests 61 through 72 is:

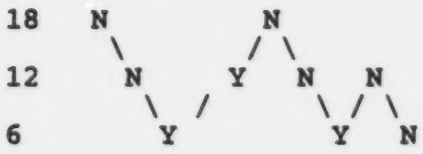

The first test was taken at a gap distance of 18 inches (45.7 cm) and it failed, so did the second test at 12 inches (30.5 cm) and so on. The ninth and last test was performed at a 6 inch (15.2 cm) gap distance and the receptor charge failed.

To calculate the P50 gap distance:

N^1 = 9 total tests

N = 9 -(2 alike initial tests - 1) = 8 nominal tests (>6)

Xf = 6 inches, is the final test distance

d = 6 inches, difference between consecutive test levels

N_Y = 3 positive responses

N_N = 5 failures excluding the first alike test

$N_N - N_Y$ = 2

From Table 5[4] A and C can be found to be -3.20 and -.10 respectively.

The sum of the test distances, Σxi, can be calculated:

Σxi = (2-1)(18 in) + 4(12 in) + 3(6 in) = 84"

Now, equation 3.2 can be used to calculate the P50 gap distance:

$$P50 = \frac{\Sigma xi}{N} + \frac{d}{N}(A + C)$$

$$= \frac{84}{8} + \frac{6}{8}(-3.20 \quad -.10)$$

$$= 8.0 \text{ in. } (20 \text{ cm})$$

The techniques by which the P50 gap distances are determined have been discussed in this section. To obtain reliable data, a reliable borehole monitoring system was used.

This system, the continuous velocity of detonation probe system, is now described.

3.3 MONITORING THE DONOR AND RECEPTOR CHARGES

The continuous velocity of detonation probe cable system is used to observe the detonation of the donor charge and monitor the gap between charges and the detonation or failure of the receptor charge.

The velocity probe comprises a length of insulated nichrome wire around which copper wire is wrapped. The nichrome wire is of constant resistance per unit length. One end of the copper wire is attached to the nichrome wire to make an electrical connection and the other end is attached to one lead of coaxial cable. The nichrome wire is attached to the other lead of the coaxial cable. The coaxial cable supplies current to the probe from a constant current source.

An oscilloscope is connected in parallel to both the constant current source and the probe for recording the resulting voltage vs. time trace on polaroid film with the aid of an oscilloscope camera.

Triggering is achieved through use of a trigger circuit so that upon blasting cap detonation the oscilloscope will start its time sweep.

At detonation the probe is shortened by ionization in the detonation head. As it is shortened the resistance across

the probe decreases. The current supplied to the probe remains constant and there is a corresponding drop in voltage. The voltage drop versus time is displayed on the oscilloscope. Knowing the full voltage drop across the probe and the length of the probe the voltage drop can be converted to distance along the charge.

Since the sweep time of the oscilloscope is known, the slope of the oscilloscope record can be used to calculate the velocity of detonation at any point along the charge from the following formula:

$$\text{velocity of detonation} = \frac{\Delta V}{\Delta T} \frac{L}{V} \qquad (3.3)$$

where: $\frac{\Delta V}{\Delta T}$ = slope of the voltage time record at any point

L = probe length

V = full voltage drop across the probe

Figure 7 is a schematic representation of the system.

The above system has many advantages. It is accurate and provides the ability of observing the detonation from the point of initiation to the end of the charge. An increasing slope on the oscilloscope record indicates a build up in the velocity of detonation. A decreasing slope indicates a failing

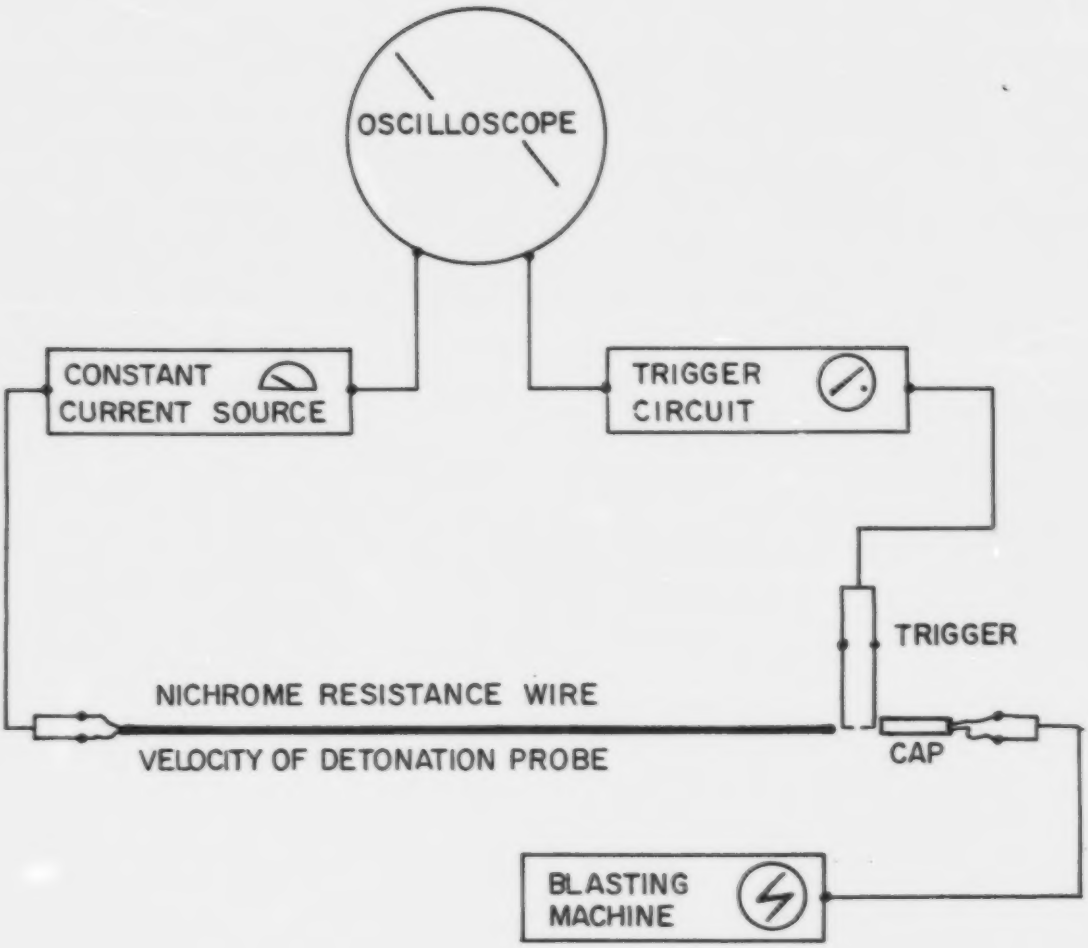

FIGURE 7 : BLAST MONITORING SYSTEM .

detonation. Also gaps in the explosive column show as an interruption in the donor charge's slope. If the receptor charge detonates, this slope resumes at a later time and closes the circuit further along the probe resulting in an instantaneous drop in voltage. If the receptor charge fails to be initiated then this second sloped line is not present.

A diagram of a fully coupled air gap test in a granite borehole is presented in Figure 8. The corresponding oscilloscope photographic record is also included. As can be seen from the photograph, the receptor charge detonated and from a plotter output of this record, the velocity of detonation for the donor charge can be calculated. Appendix C contains the plotter output for this test and illustrates the method of calculating the donor charge's velocity of detonation. Ideally, for more accurate V.O.D. determination, the explosive column should have no interruption so that a longer trace may be obtained. The detonation velocities of the receptor charges were not calculated since inaccuracies arise when the shockwave and expanding gases from the donor detonation cause the receptor to move.

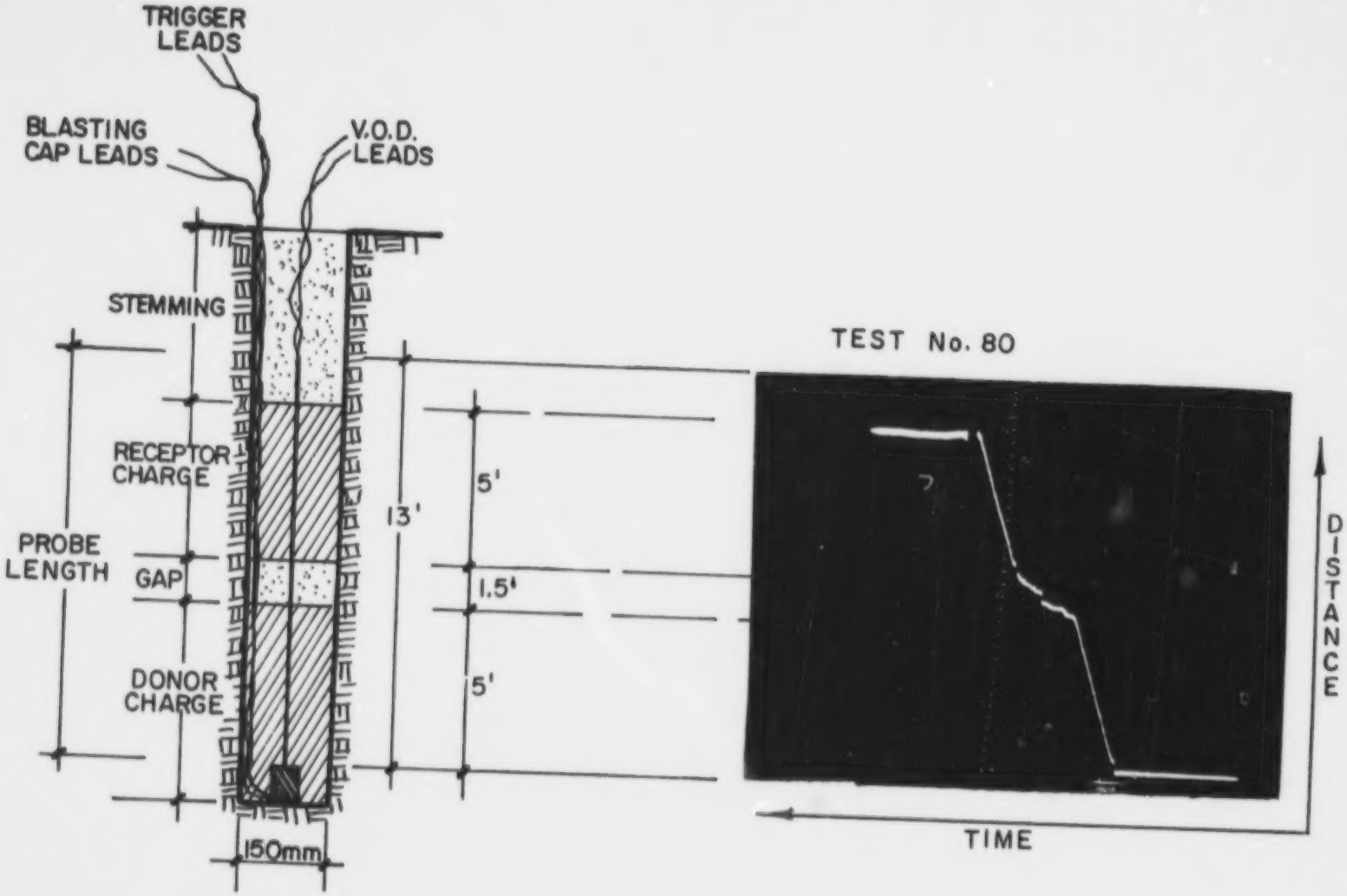

FIGURE 8 : DETERMINATION OF RECEPTOR DETONATION OR FAILURE USING THE PROBE CABLE METHOD.

CHAPTER 4

EXPERIMENTAL

4.0 INTRODUCTION

The explosives used for sand gap testing are listed in Table 6 along with the hole diameters and mode of hole loading. The average donors velocity of detonation is also given in this table. Appendix D lists the trade names of the explosives tested.

Three areas of fully coupled sand gap testing at 20°C are investigated. These are:

1) Sand Gap Tests for Non-cap Sensitive Products A, B, C and AN/FO.
2) Sand Gap Tests for Non-cap Sensitive Product C When the Receptor Charge Contains a Non-electric Cap and/or Cast Primer.
3) Sand Gap Tests for Cap Sensitive Product D.

For the non-cap sensitive products the P50 sand gap distance, gap distance at which the probability of cross-propagation is 50%, is determined for each product at 90 mm and 150 mm charge diameters. The P05 and P95 sand gap distances are estimated for each of these products also.

EXPLOSIVE	EXPLOSIVE DIAMETER (mm)	AVERAGE DONOR VELOCITY OF DETONATION (km/s)	HOLE DIAMETER (mm)	METHOD OF CHARGING THE HOLE
PRODUCT A	75	4.39	90	
	125	4.48	150	
PRODUCT B	75	4.24	90	LIGHTLY TAMPED IN PLACE TO FILL THE BOREHOLE
	125	5.55	150	
PRODUCT C	75	5.61	90	
	125	6.10	150	
PRODUCT D	40	3.75	50	
	50	4.11	90	
	50	4.88	150	BUNDLED AND LIGHTLY TAMPED TO FILL THE BOREHOLE
AN/FO	90	3.35	90	FREE POURED
	150	3.47	150	

TABLE 6: THE EXPLOSIVES AND DIAMETERS TESTED.

The P50 sand gap distance is then determined for Product C at 90 mm and 150 mm charge diameters when a non-electric cap and cast primer are placed in the receptor charge. P05 and P95 sand gap distances are estimated also. The results obtained are compared to results of tests with a cast primer in the receptor charge, and no cap or primer in the receptor charge.

The P50 sand gap distance is also determined for cap sensitive Product D at 50 mm, 90 mm and 150 mm charge diameters. The P05 and P95 sand gap distances are estimated for this product also. The results are compared to anticipated results reported previously for similar cap sensitive products.

4.1 SAND GAP TESTS FOR NON-CAP SENSITIVE PRODUCTS A, B, C AND AN/FO

Figures 9 and 10 are illustrations of the test set-ups for 90 mm and 150 mm diameter borehole tests in granite.

Appendix E contains the resultant "up-and-down" receptor result plots for tests on 90 mm diameter Product A, B, C and AN/FO charges respectively. The P50 sand gap distances calculated for these products are shown on their respective "up-and-down" plots and are contained in Table 7.

Appendix F contains the resultant "up-and-down" receptor result plots for tests on these products at a 150 mm charge diameter. The P50 results are illustrated in the Appendix and are contained in Table 7.

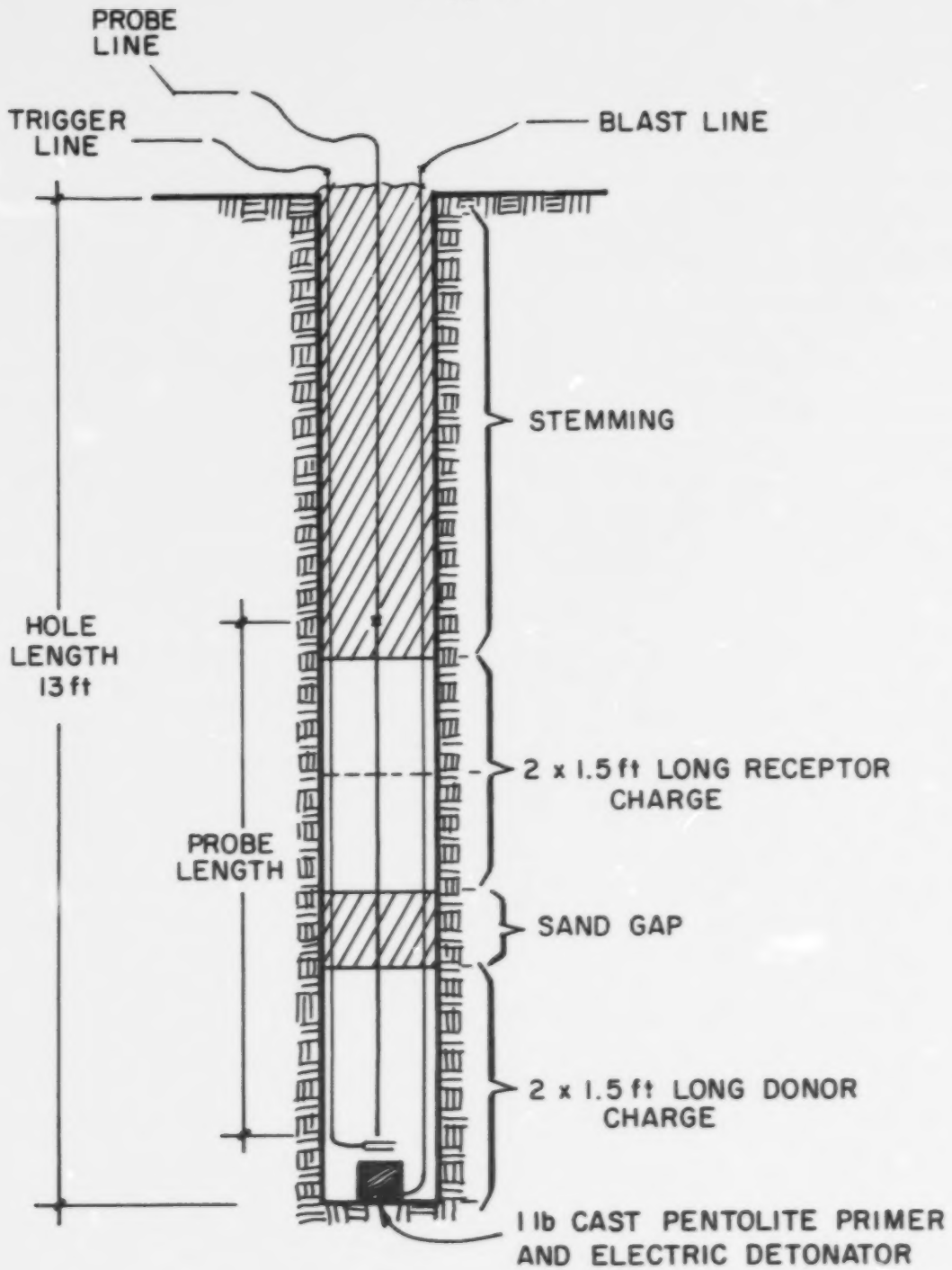

FIGURE 9 : CROSS SECTION OF A 90mm DIAMETER TEST HOLE.

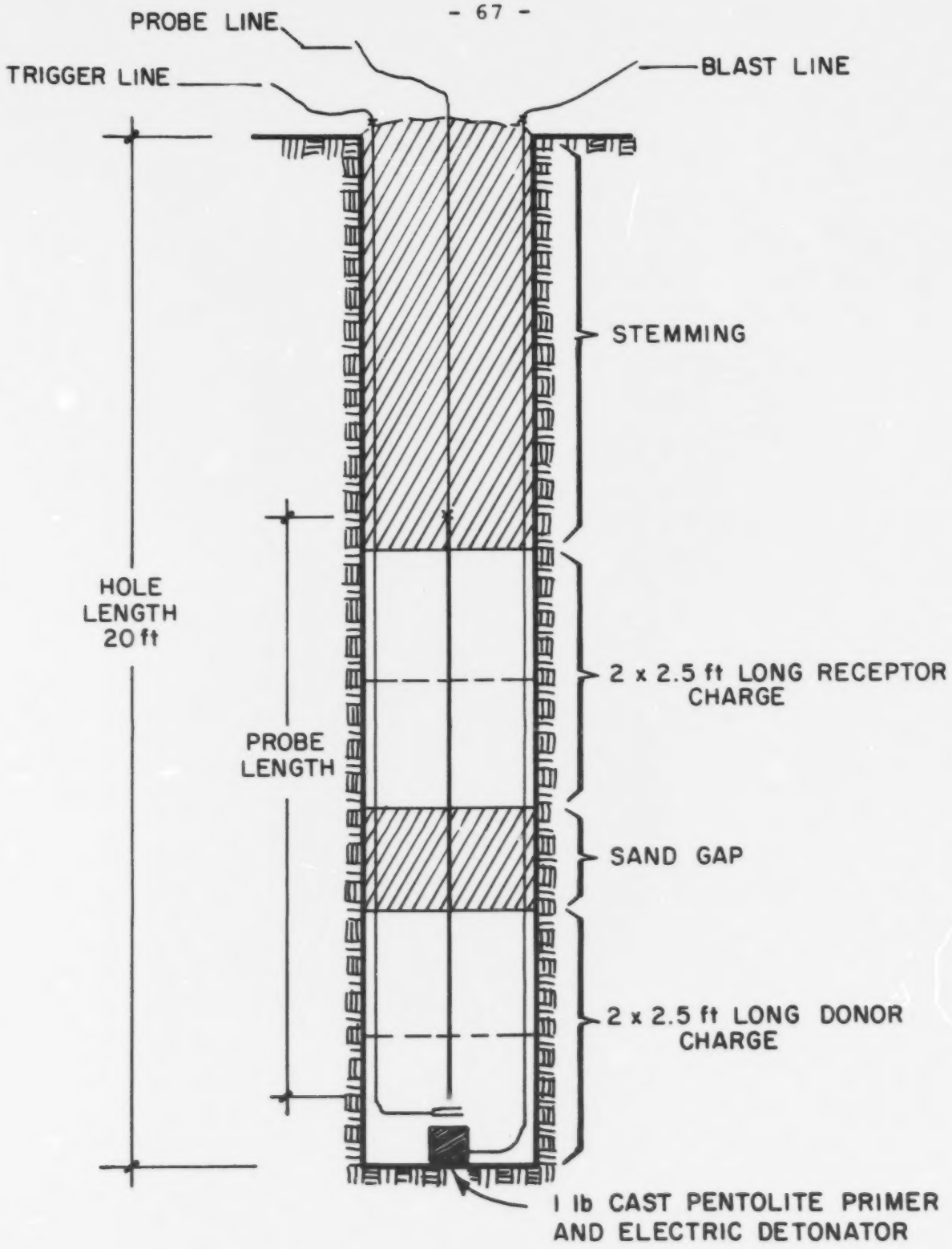

FIGURE 10 : CROSS SECTION OF A 150mm DIAMETER TEST HOLE.

PRODUCT	CHARGE DIAMETER (mm)	SAND GAP DISTANCE ESTIMATED P95 (cm)	SAND GAP DISTANCE CALCULATED P50 (cm)	SAND GAP DISTANCE ESTIMATED P05 (cm)
A	90	5	24	35
	150	20	39	70
B	90	0	4	15
	150	0	20	45
C	90	0	9	20
	150	30	55	80
AN/FO	90	5	26	40
	150	40	67	100

TABLE 7: SAND GAP DISTANCES FOR NON-CAP SENSITIVE PRODUCTS CALCULATED AT 50% AND ESTIMATED FOR 5 AND 95% PROBABILITY OF CROSS-PROPAGATION.

Table 7 also contains the estimated P05 and P95 sand gap distances for all of these tests. These P05 and P95 distances are estimated from the "up-and-down" plots in Appendices E and F.

The P50, P95 and P05 sand gap distances in Table 7 are plotted versus charge diameter in Figures 11, 12 and 13 respectively.

The P50 sand gap distances cross-propagated for the non-cap sensitive products are shorter than those predicted by the scaling relations developed in the 1985 report[1]. This can be expected however due to the fact that the 1985 report dealt with cap sensitive products and the products tested thus far here are considered non-cap sensitive. Although the product families may be manufactured roughly the same, the sensitivity of the products is decreased at charge diameters greater than 75 mm.

Figure 12 indicates that all of the products considered have poor sand gap cross-propagation properties at a 90 mm charge diameter. At this diameter cartridged products should be loaded carefully to avoid trapping sand or drill cuttings between successive cartridges.

At a 150 mm charge diameter Product B, believed to be air bubble sensitized, shows an extremely poor sand gap cross-propagation sensitivity. In the 1985 report[1] it was noted that some receptor products of this type may have initiation properties very sensitive to a decrease in the amount of hot

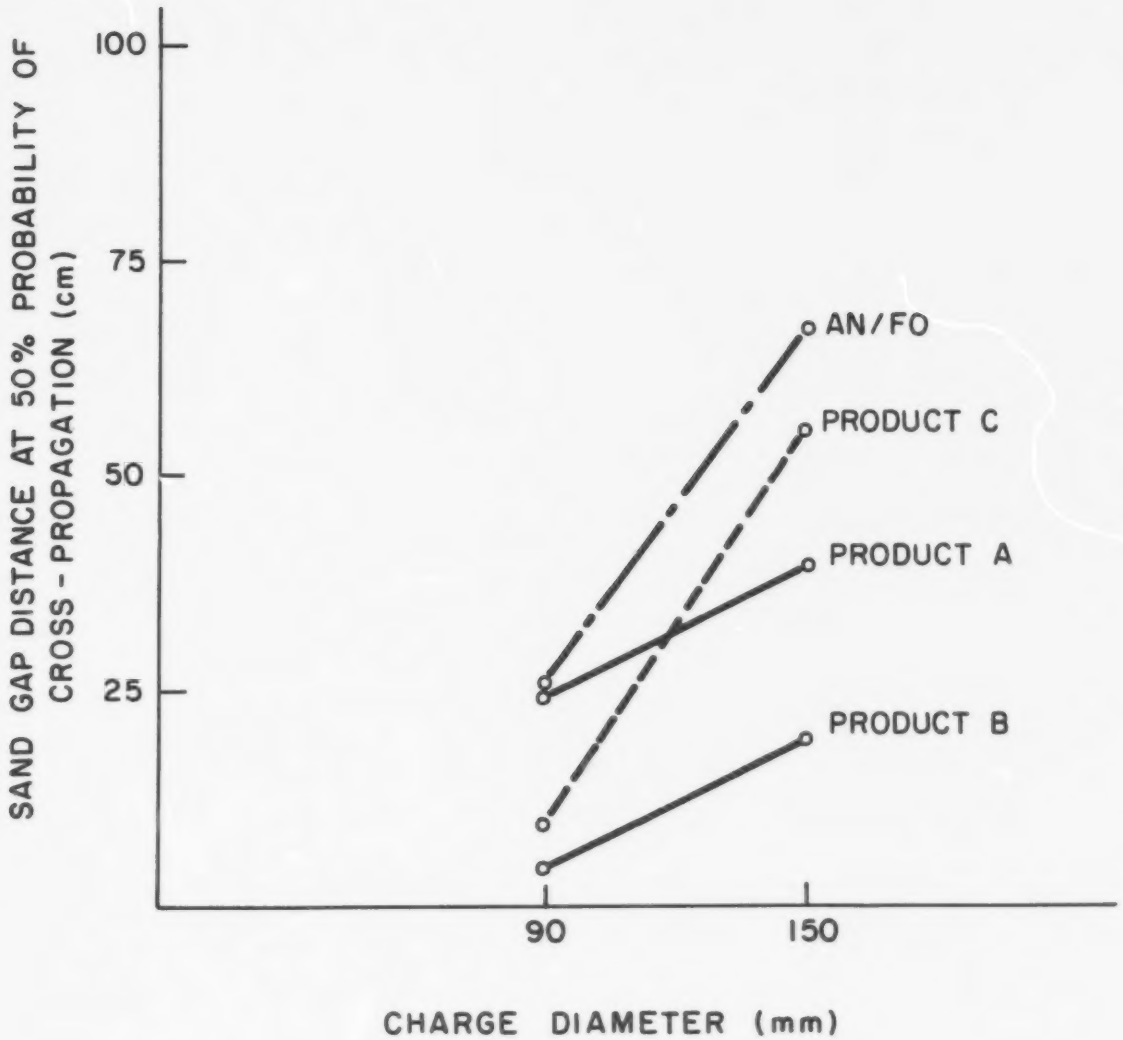

FIGURE 11 : SAND GAP DISTANCE VERSUS CHARGE DIAMETER FOR NON-CAP SENSITIVE PRODUCTS AT 50% PROBABILITY OF CROSS-PROPAGATION.

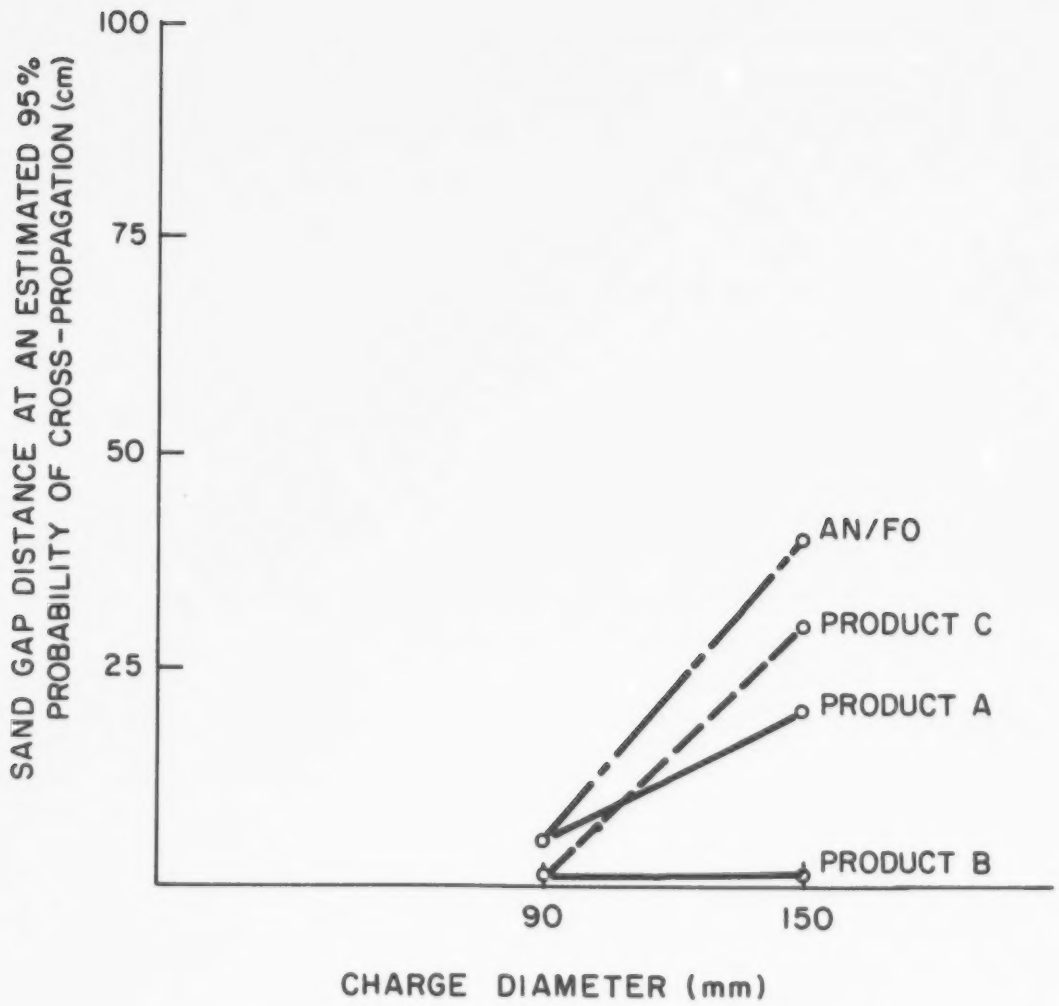

FIGURE 12 : SAND GAP DISTANCE VERSUS CHARGE DIAMETER FOR NON-CAP SENSITIVE PRODUCTS AT AN ESTIMATED 95% PROBABILITY OF CROSS-PROPAGATION.

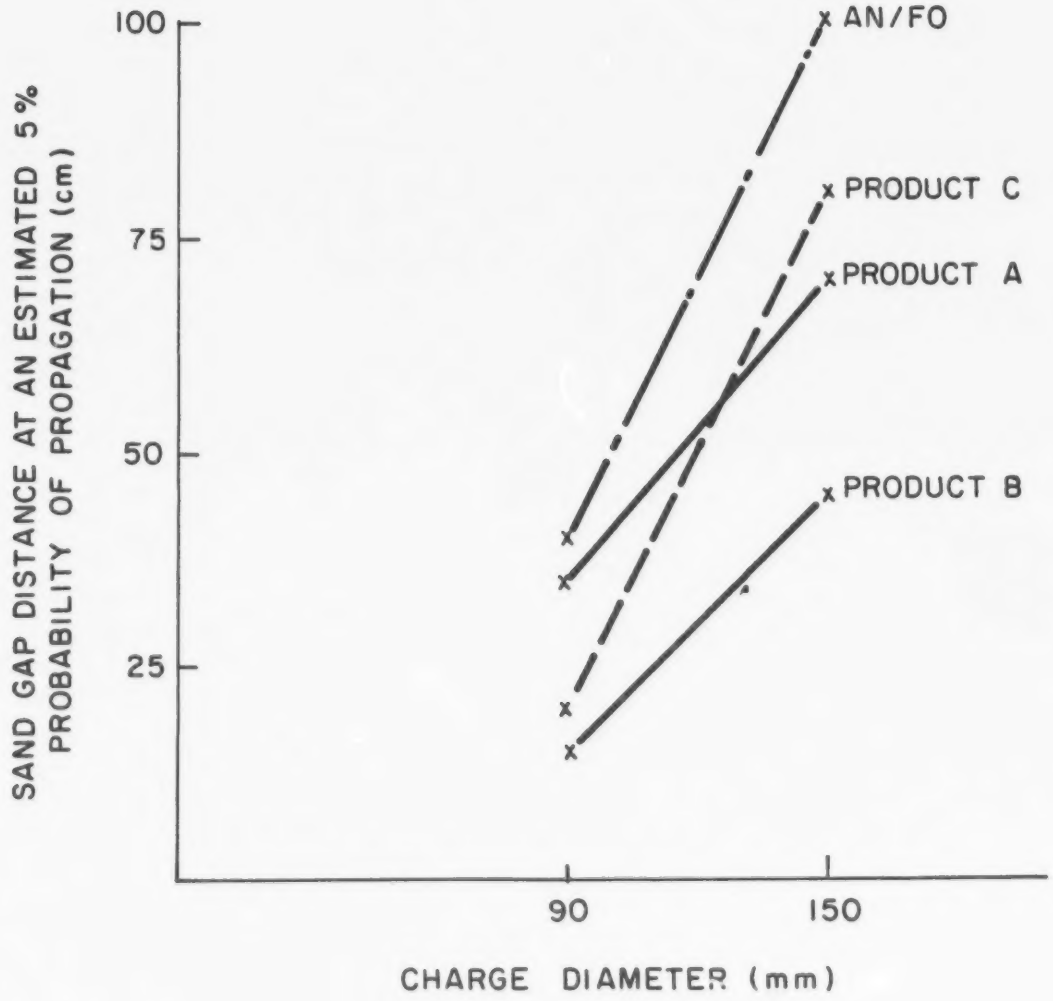

FIGURE 13 : SAND GAP DISTANCE VERSUS CHARGE DIAMETER FOR NON-CAP SENSITIVE PRODUCTS AT AN ESTIMATED 5% PROBABILITY OF CROSS-PROPAGATION.

products impacting them from the donor charge. In this study, with sand as the gap medium, the hot products from the donor charge would be impeded before reaching the receptor charge.

From Figure 13 it is evident that for a 150 mm charge diameter one would not expect a cross-propagation over 100 cm for any of the products. This sand distance is shorter than those known to be cross-propagated in decked hole blasting operations. These larger distances could be due to shock initiation of the blasting cap or cast primer in the receptor charge rather than initiation of the explosive charge itself. The phenomena of initiation of primed receptor charges is investigated in the following section.

4.2 SAND GAP TESTS FOR NON-CAP SENSITIVE PRODUCT C WHEN THE RECEPTOR CHARGE CONTAINS A BLASTING CAP AND/OR CAST PRIMER

Figure 14 illustrates the test set-ups for a typical sand gap test when the receptor charge contains a primer and blasting cap. The non-electric cap type tested had a No. 1 short period delay of 30 ms. This delay was chosen so that the oscilloscope could monitor the receptor charge initiation whether the donor initiated the cap directly or the delay element in the cap.

Appendix G contains the resultant "up-and-down" receptor result plots for tests on the 90 mm and 150 mm diameter Product C with a cap and a cast primer in the receptor charge.

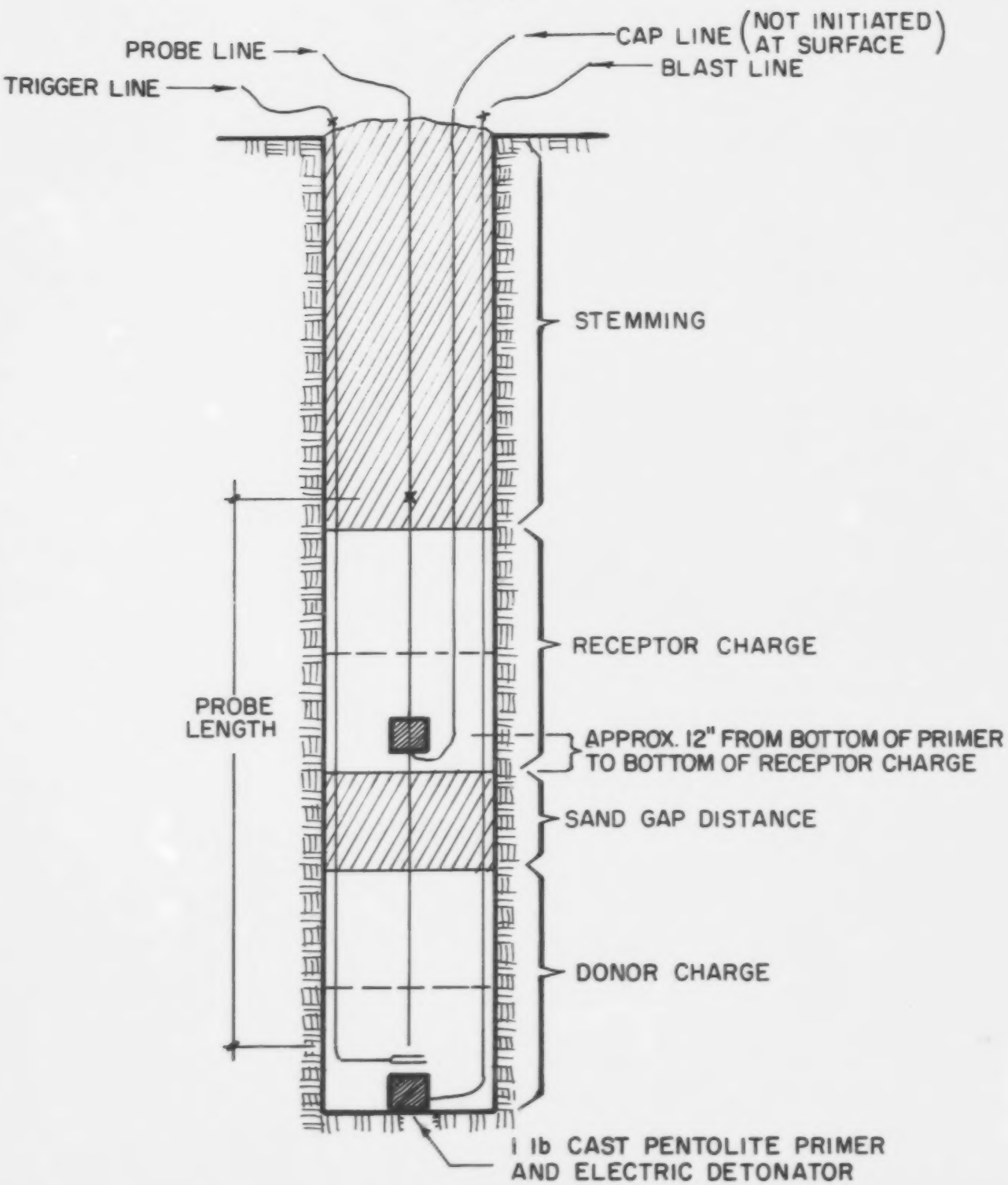

FIGURE 14 : CROSS SECTION OF A TEST HOLE ILLUSTRATING THE BLASTING CAP AND PRIMER POSITION IN THE RECEPTOR CHARGE.

Table 8 contains the calculated P50 and estimated P05 and P95 sand gap distances cross-propagated. For comparison, the results obtained when there was no cap or primer in the receptor charge are included in this table also. Figure 15 is a graphical comparison of the two sets of results. It is evident that either the cap or the cast primer in the receptor charge is more sensitive to detonation than the Product C itself.

Two additional tests at 90 mm charge diameter were performed at a sand gap distance of 1.0 feet (≈ 30 cm). At this gap distance the Product C as the receptor charge will not detonate, but if a cap and primer are placed in the receptor charge the receptor will detonate. The receptor charge in these two tests contained a cast 1 lb. primer with no blasting cap. In these two tests the receptor charge failed to detonate thereby it is apparent that it is the non-electric cap which is responsible for receptor detonation when it is primed.

4.3 SAND GAP TESTS FOR CAP SENSITIVE PRODUCT D

Figure 16 illustrates the test set-up for the 50 mm diameter borehole tests in granite.

Appendix H contains the resultant "up-and-down" receptor result plots for tests on Product D at charge diameters of 50, 90 and 150 mm respectively. The P50 sand gap distances calculated for these diameters are shown on their respective "up-and-down" plots and are contained in Table 9. Table 9 also

PRODUCT	RECEPTOR WITHOUT A CAP AND WITHOUT A PRIMER			RECEPTOR WITH A CAP AND WITH A PRIMER		
	ESTIMATED P95 (cm)	CALCULATED P50 (cm)	ESTIMATED P05 (cm)	ESTIMATED P95 (cm)	CALCULATED P50 (cm)	ESTIMATED P05 (cm)
C (90mm dia.)	0	9	20	40	65	90
C (150mm dia.)	30	55	80	68	99	130

TABLE 8: SAND GAP DISTANCES FOR PRODUCT C CALCULATED AT 50% AND ESTIMATED FOR 5 AND 95% PROBABILITY OF CROSS-PROPAGATION.

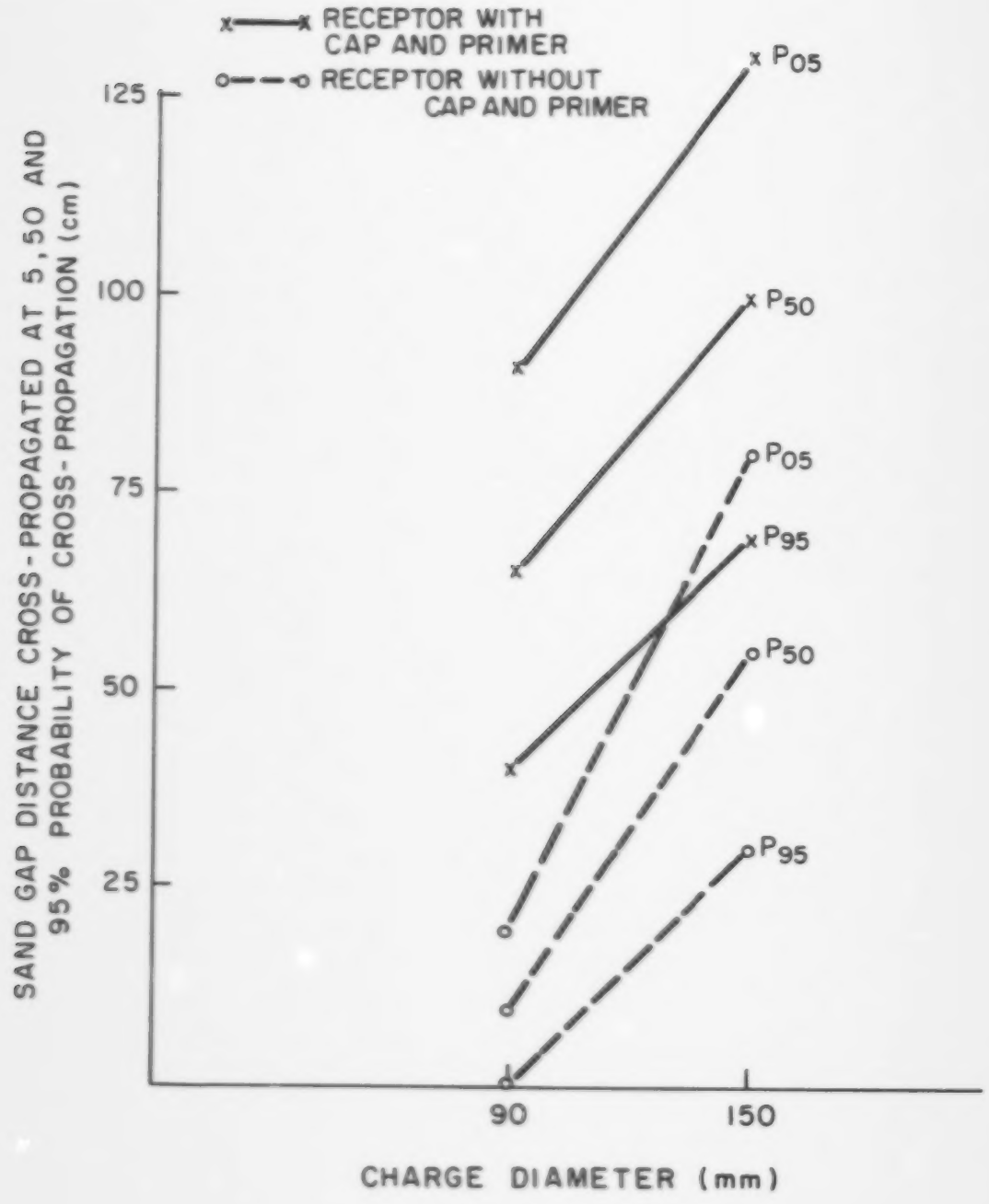

FIGURE 15 : SAND GAP DISTANCE VERSUS CHARGE DIAMETER FOR NON-CAP SENSITIVE PRODUCT C ILLUSTRATING THE EFFECT OF PLACING A CAP AND A CAST PRIMER IN THE RECEPTOR CHARGE.

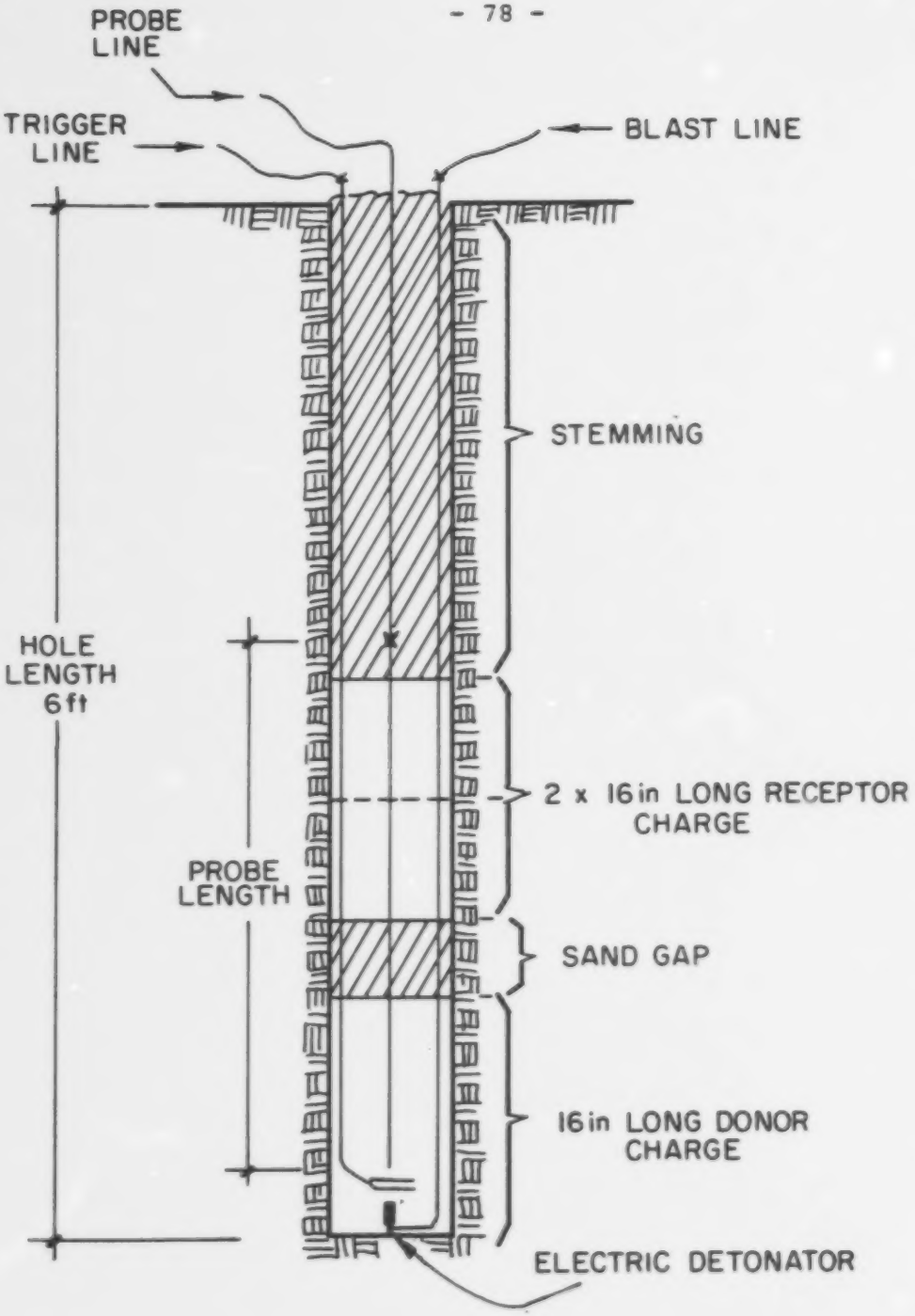

FIGURE 16 : CROSS SECTION OF A 50mm DIAMETER TEST HOLE.

PRODUCT	CHARGE DIAMETER (mm)	SAND GAP DISTANCE ESTIMATED P95 (cm)	CALCULATED P50 (cm)	ESTIMATED P05 (cm)
D	50	0	10	30
	90	10	24	40
	150	40	52	65
C	90	0	9	20
	150	30	55	80

TABLE 9: SAND GAP DISTANCES FOR PRODUCTS C AND D CALCULATED AT 50% AND ESTIMATED FOR 5 AND 95% PROBABILITY OF CROSS-PROPAGATION.

contains the estimated P05 and P95 and gap distances cross-propagated. For comparison, the results obtained from a similar non-cap sensitive product, Product C are included in this table also.

Figure 17 is a graphical comparison of the two sets of P50 results. Also included for comparison is the extrapolated cap-sensitive results for a similar product tested in the 1985 report[1].

It is evident that the gap distances cross-propagated by Product D are different than those distances extrapolated from the 1985 report[1]. This can be expected as the 1985 report dealt with a product of the same general type but produced by a different company and the results obtained were extrapolated from charge diameters of less than 50 mm.

Also, as expected, the cap sensitive Product D was more sensitive than the non-cap sensitive Product C. It is interesting to note that at a 150 mm charge diameter the gap distances cross-propagated are similar.

This could be due to the difficulties in bundling and tamping the Product D 50 mm cartridges into 150 mm diameter holes so as to act as a homogeneous 150 mm diameter charge.

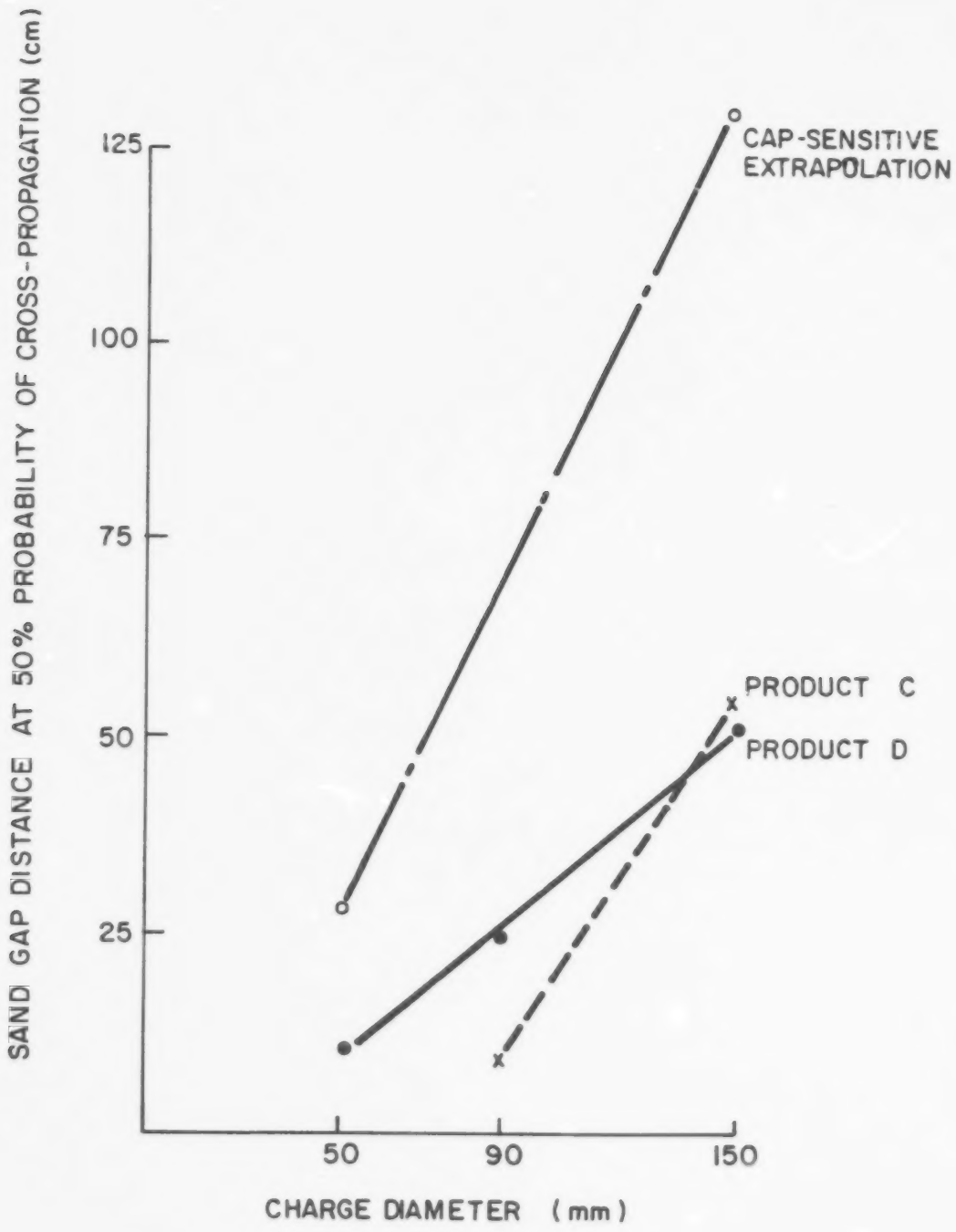

FIGURE 17 : SAND GAP DISTANCE VERSUS CHARGE DIAMETER FOR PRODUCT C AND D AND ON EXTRAPOLATION FROM THE 1985 REPORT [1].

CHAPTER 5

CONCLUSIONS

Results from traditional, laboratory scale gap sensitivity tests are of little practical use to mine operators. These tests do not take into account factors such as charge diameter and confinement, both of which have a great influence on the detonation and the sensitivity of explosives. The effect of gap material such as sand is not usually considered by these traditional gap sensitivity tests but these gap mediums can be common in mine blasting situations.

Insitu sand gap tests in 90 mm and 150 mm diameter boreholes on typical commercial explosives have revealed the sand gap distances cross-propagated at 50% probability of cross-propagation for the products considered. These results also allowed the sand gap distances cross-propagated at a high and low probability of cross-propagation to be estimated.

AN/FO in 150 mm holes appears to be able to cross-propagate sand gap distances less than 40 cm all of the time while not being able to cross-propagate sand gap distances greater than 1 m at any time. AN/FO is more sensitive than the other products tested.

The results of testing indicated that the sand gap distances cross-propagated were less than those cross-propagated in deck blasting operations. This was found to be due to the sensitivity of the non-electric cap in the primer of the receptor charge. Further work should be performed to optimize the type of non-electric cap to be used in deck blasting operations.

This research provided sand gap performance data for several commercial explosives. It also indicated that cross-propagation between explosive decks is due to the sensitivity of the blasting cap in the subsequent deck rather than due to the sensitivity of the explosive or primer itself. A blasting cap with a reduced sensitivity would prove beneficial in that it would allow more flexibility when designing deck intervals for large diameter hole stoping operations.

REFERENCES

1. Bauer, A.W., Bauer, A.: Evaluation of Propagation Sensitivity of Commercial Explosives. Canmet Project No. 220102, February 1985.

2. Dixon, W.J.: The Up-and-Down Method for Small Samples. J. Am. Stat. Assoc. V. 60, pp. 967 - 978.

3. Brownlee, K.A. et. al.: The Up-and-Down Method with Small Samples. J. Am. Stat. Assoc., v. 48, pp. 262 - 277.

4. Dixon, W.J., and Massey, F.M.: Introduction to Statistical Analysis. McGraw-Hill Book Co. Inc., New York, 2nd Ed., (1957), pp. 488. (Personal Telephone Interview - August 1986)

5. Bowden, F.P., Yoffee, A.D.: Initiation and Growth of Explosion in Liquids and Solids. Cambridge Monographs on Physics, The Cambridge University Press, London (1952).

6. Mader, C.L.: Los Alamos Explosives Performance Data. Berkeley, University of California Press, London (1952)

7. Winning: 2nd Office of Navel Research Symposium on Detonation. Washington, D.C., (1955).

8. King, A.W.: Shock Characteristics of Ammonium Nitrate. M.Sc. Thesis, Queen's University at Kingston (1979).

9. Bruckmann, H.J., Guillet, J.E.: Theoretical Calculations of Hot-Spot Initiation in Explosives. Canadian Journal of Chemisty, 46, 3221 (1968).

10. Tulis, A.J., Austing, J.L., Baker, D.E.: Open Matrix Very Low Density Explosive Formulations. Journal of Hazardous Materials, 5 (1982).

11. Cook, M.A.: The Science of High Explosives. American Chemical Society Monograph Series, Reinhold Book Corporation, New York (1958).

12. Taylor, J.: Detonation in Condensed Explosives. Clarendon Press, Oxford (1952).

13. Lewis, B, von Elbe, G.: Combustion Flames and Explosives of Gases. Academic Press Inc., New York and London, (1961).

14. Griffith, W.: Various Papers, The Journal of Explosives Engineering (1985).

15. Bauer, A.: Explosives Technology. Published notes for Mining Engineering Course - Mine 220. Department of Mining Engineering, Queen's University at Kingston (1981).

16. Katsabanis, P.: A Comparative Study of Emulsion and Slurry Explosives. M.Sc. Thesis, Queen's University at Kingston (1983).

APPENDIX A

SAMPLE CALCULATION OF THE FINAL TEMPERATURE REACHED IN NON-GASSED NITROMETHANE UNDER SHOCK

PERTINENT NITROMETHANE DATA

Density, $\rho_1 = 1.14$ g/cc

Specific volume, $V_1 = 0.88$ cc/g

Specific heat, $C = 0.412$ cal/g/°K

Assume the nitromethane is shocked at a shock velocity, $D = 3000$ m/s

The relationship between shock velocity and particle velocity, W, for nitromethane from equation 2.20 is:

$$D = 1647 + 1.637\,W$$

therefore: $W = 824$ m/s

The pressure reached by the nitromethane under this shock is given by equation 2.16:

$$P_2 = \rho_1 DW$$

therefore: $P_2 = (1.14 g/cm^3)(3000 m/s)(824 m/s)(10^6 cm^3/m^3)$

$= 2.8181 \times 10^{12}$ g/ms^2

$= (2.8181 \times 10^9$ kg/ms$^2) \times (1/9.81$ s^2/m)

$= 2.8727 \times 10^8$ kg/m^2

$$= 2.8727 \times 10^4 \text{kg/cm}^2 \times (.98060 \text{ bars}/(\text{kg/cm}^2))$$

$$P_2 = 28.17 \text{ Kbars}$$

The specific volume, at this pressure, V_2, is given by equation 2.15:

$$V_2 = (-W/D + 1)V_1$$

$$V_2 = V_1 - V_1 W/D$$

$$= 0.88 \text{ cc/g} - (0.88 \text{ g/cc})(824 \text{ m/s})/(3000 \text{ m/s})$$

$$= 0.638 \text{ cc/g}$$

The change in energy, $E_2 - E_1$, is given by equation 2.18:

$$E_2 - E_1 = \tfrac{1}{2} P_2(V_1 - V_2)$$

$$= (.5)(28170\text{bars})(.242\text{cm}^3/\text{g}) \times (1.0197(\text{kg/cm}^2)/\text{bar})(.01 \text{ m/cm}) \times (9.81 \text{ m/s})$$

$$= 340.97 \text{ kgm}^2/\text{gs}^2$$

$$= 340.97 \text{ J/g} \times .239 \text{ cal/J}$$

$$E_2 - E_1 = 81.28 \text{ cal/g}$$

The change in temperature, $T_2 - T_1$, is given by equation 2.19:

$$T_2 - T_1 = (E_2 - E_1)/C$$

$$= (81.28 \text{ cal/g})/.412 \text{ cal/g/°K}$$

$$T_2 - T_1 = 197.27°K$$

Therefore the nitromethane is bulk heated to a temperature, T_2 given by:

$$T_2 = (T_2 - T_1) + T_1$$

$$= (197.27°K) + 288°K$$

$$T_2 = 485°K$$

where T_1 is the initial nitromethane temperature before the shock.

APPENDIX B

SAMPLE CALCULATION OF THE FINAL TEMPERATURE REACHED IN AN AIR BUBBLE UNDER SHOCK

For nitromethane containing air bubbles:

Initial temperature of the air bubble, T_1 = 288°K

Initial pressure in the air bubble, P_1 = 1.013 bars

The ratio of specific heats for air, γ = 1.4

Assume the shock velocity in the nitromethane is 3000 m/s as in the bulk heating case in Appendix A.

The pressure in the air bubble in question will rise to P_2 = 28170 bars.

The final temperature in the air bubble under this pressure increase is given by equation 2.21:

$$T_2 = T_1 \left(\frac{P_2}{P_1}\right)^{[(\gamma-1)/\gamma]}$$

$$= (288°K) \left(\frac{28170 \text{ bars}}{1.013 \text{ bars}}\right)^{(.4/1.4)}$$

$$T_2 = 5360°K$$

APPENDIX C

ILLUSTRATION OF CALCULATION THE DONOR CHARGE VELOCITY OF DETONATION

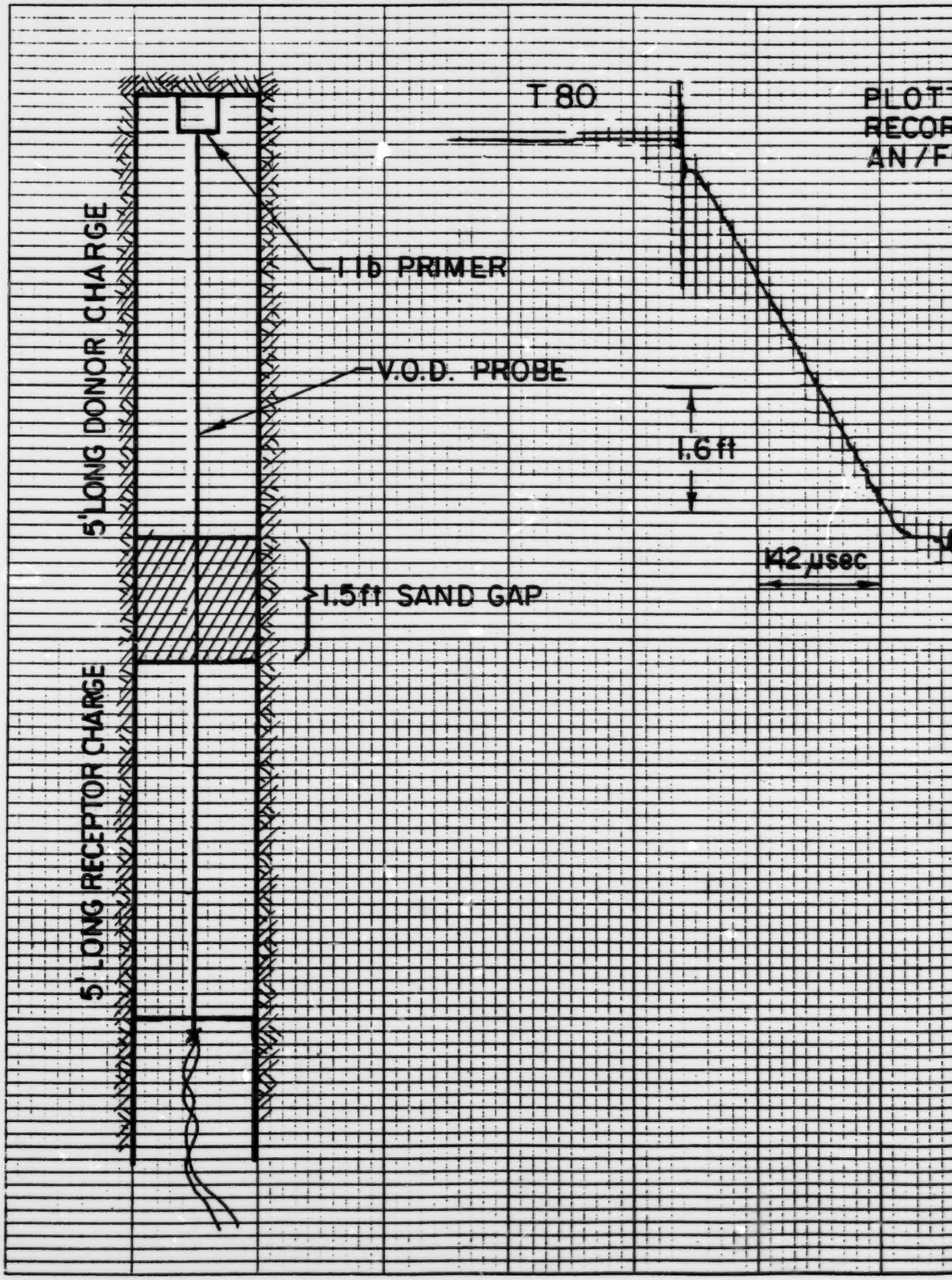
5' LONG DONOR CHARGE
1 lb PRIMER
V.O.D. PROBE
1.5 ft SAND GAP
5' LONG RECEPTOR CHARGE
T 80
1.6 ft
142 μsec

ER VELOCITY OF DETONATION
O FOR 150 mm DIAMETER
SAND GAP TEST
TEST No. 80

OONOR V.O.D. = 11300 ft/sec
= 3440 m/sec

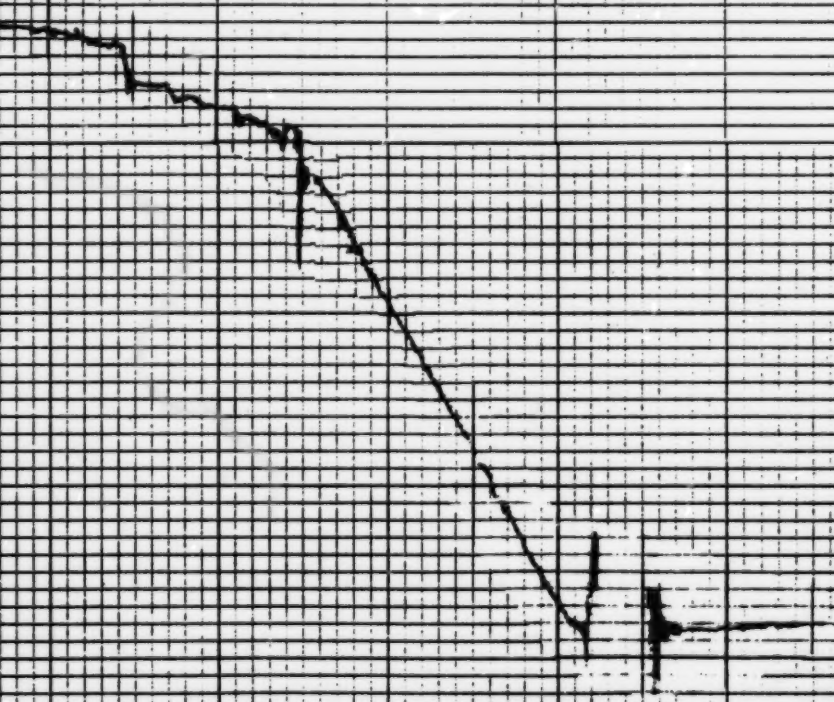

K+E 10 X 10 TO THE INCH • 10 X 15 INCHES
KEUFFEL & ESSER CO. MADE IN U.S.A.
47 0700

APPENDIX D

TRADE NAMES OF THE EXPLOSIVES TESTED

APPENDIX E

"UP-AND-DOWN" RECEPTOR RESULT PLOTS FOR 90 MM DIAMETER

PRODUCT A, B, C AND AN/FO CHARGES

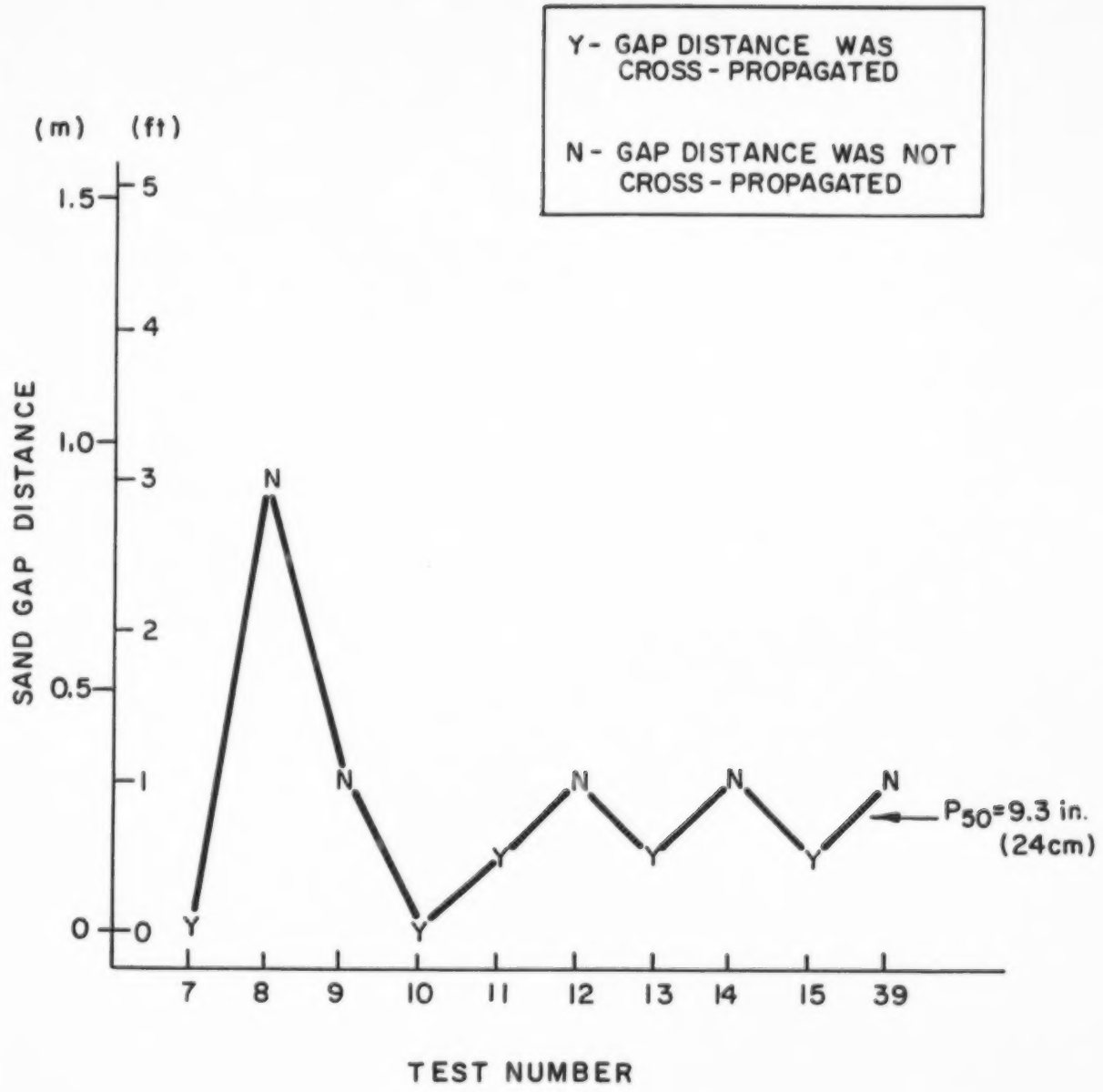

PRODUCT A — 90mm DIAMETER

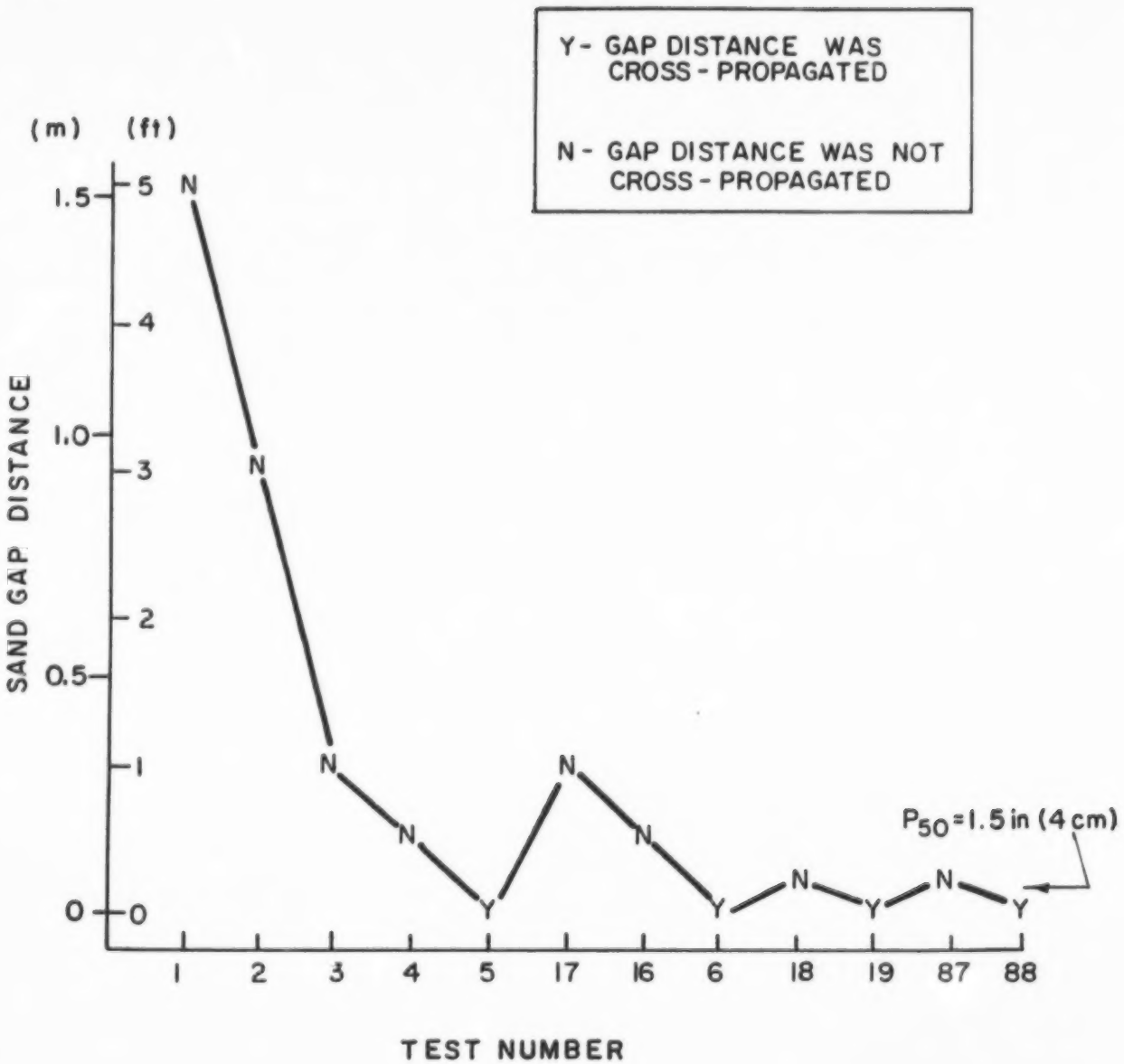

PRODUCT B – 90 mm DIAMETER

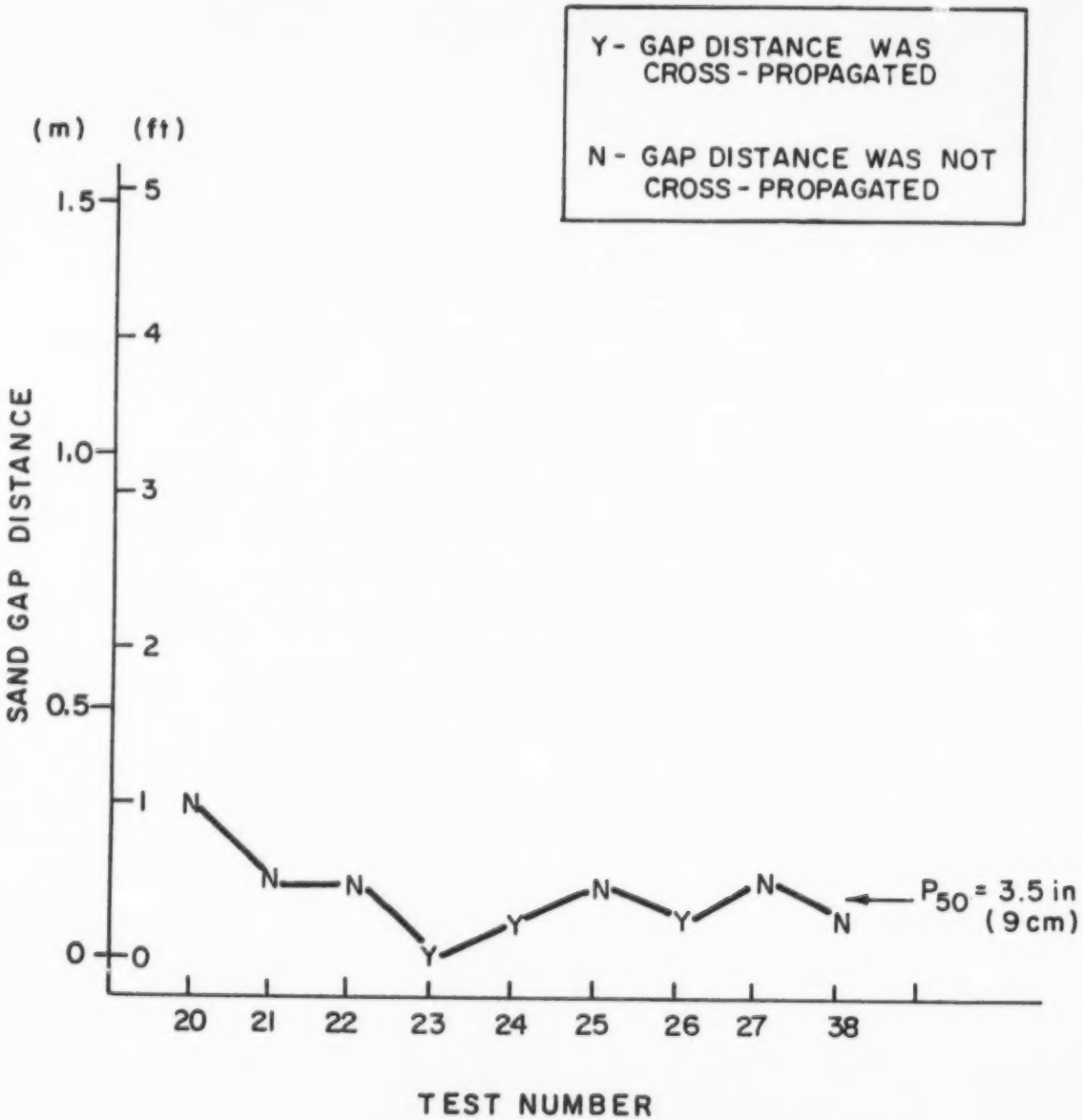

PRODUCT C – 90mm DIAMETER

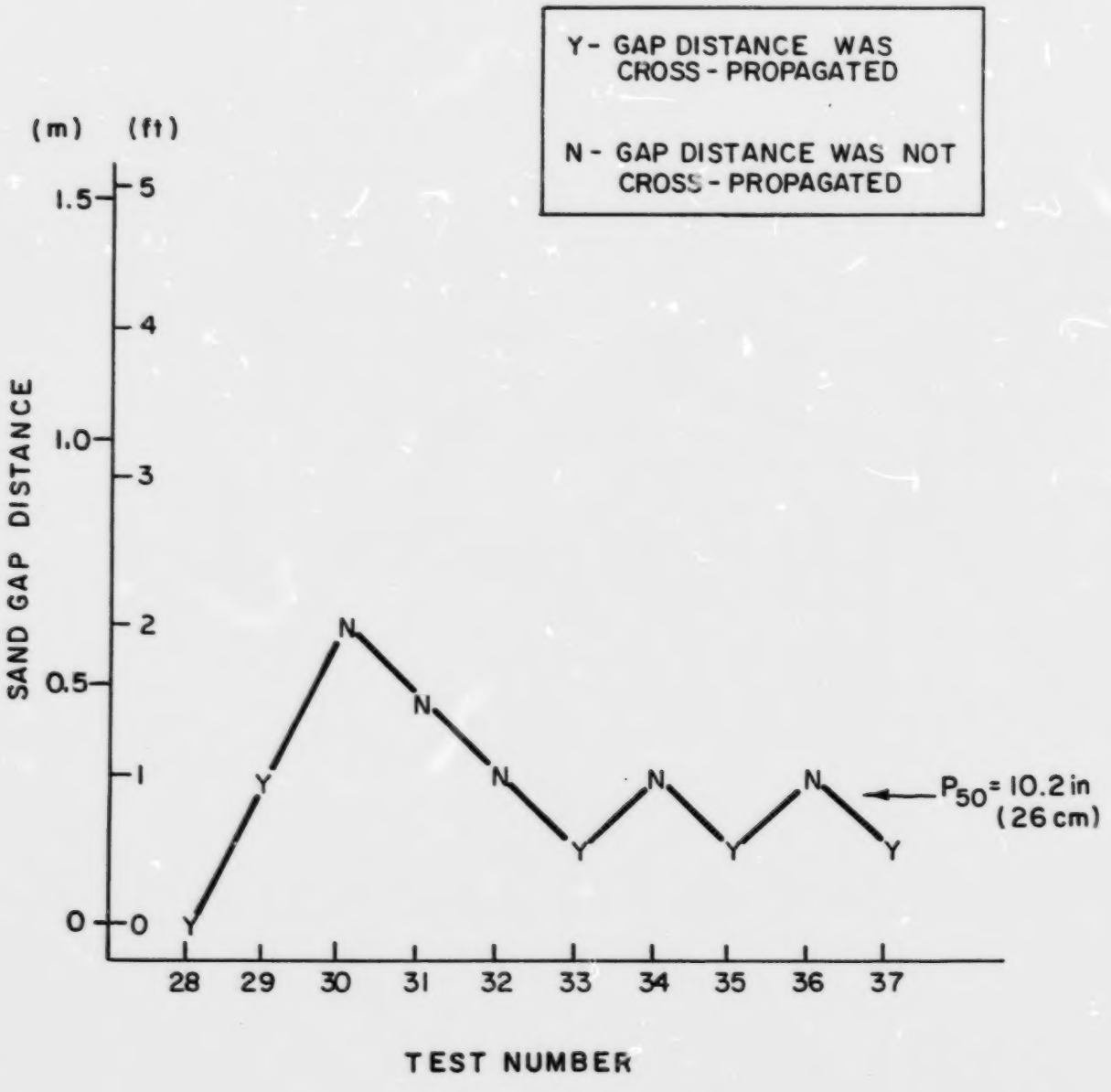

AN/FO – 90mm DIAMETER

APPENDIX F

"UP-AND-DOWN" RECEPTOR RESULT PLOTS FOR 150 MM DIAMETER

PRODUCT A, B, C AND AN/FO CHARGES

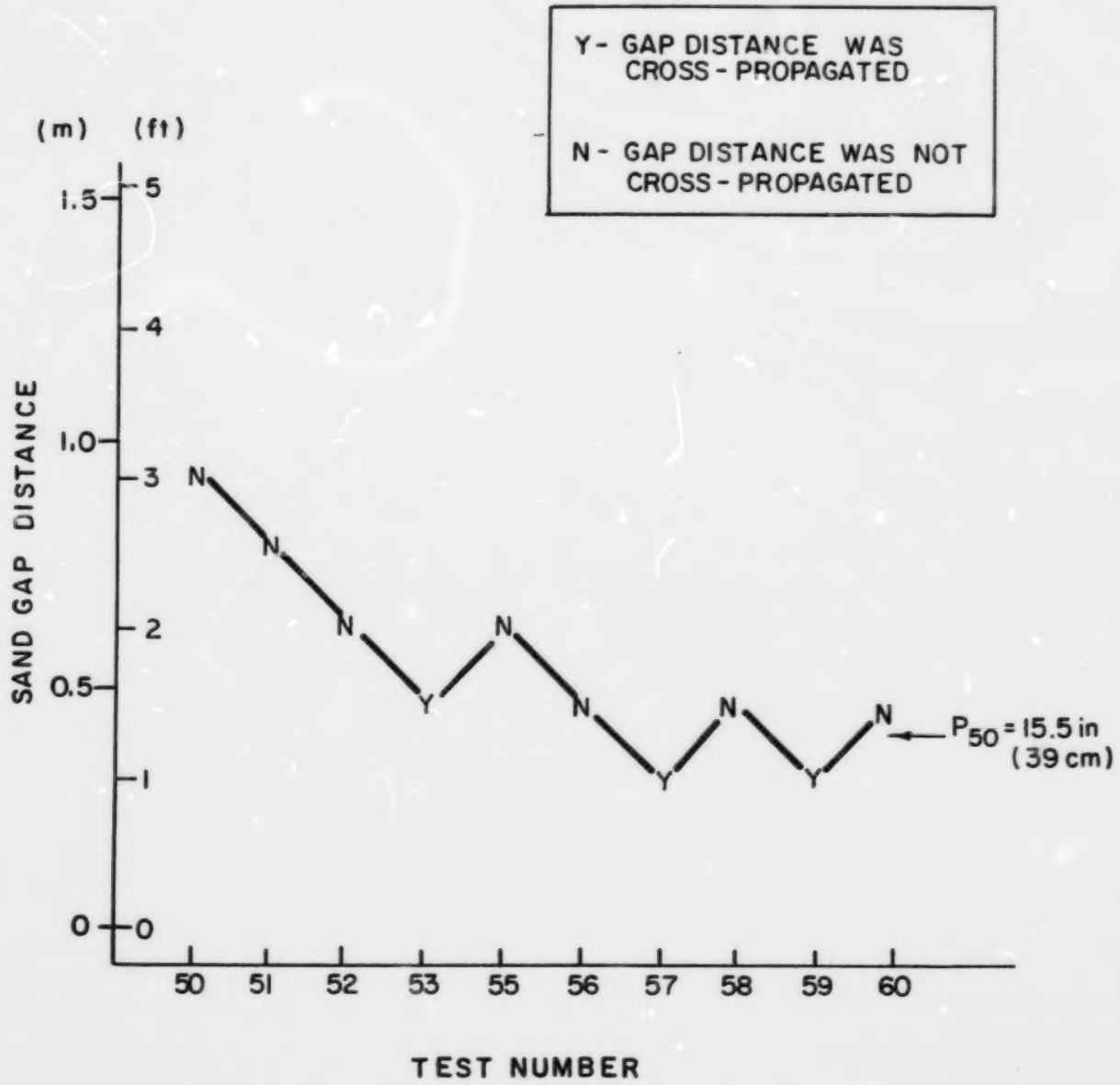

PRODUCT A – 150mm DIAMETER

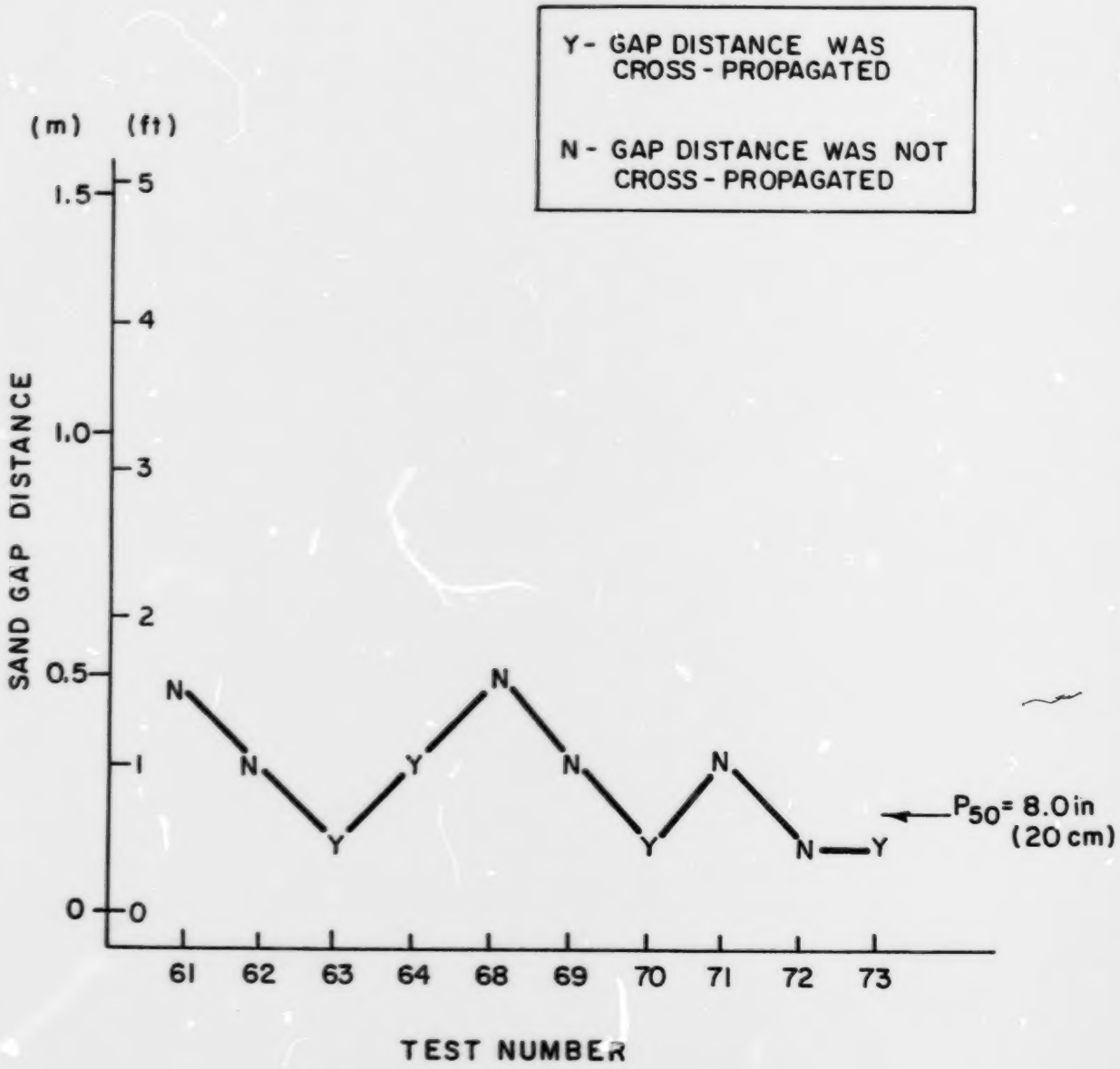

PRODUCT B – 150mm DIAMETER

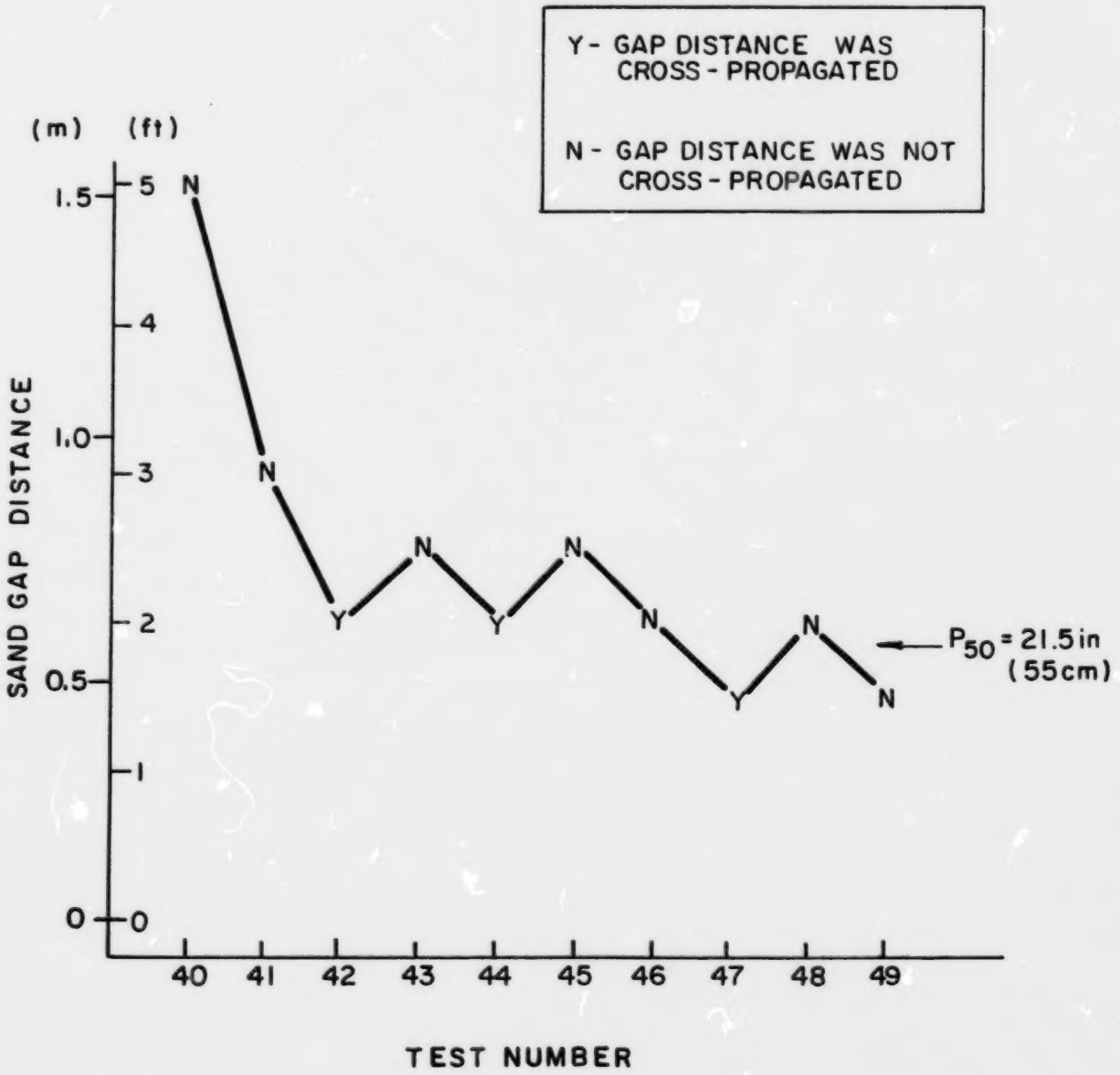

PRODUCT C – 150mm DIAMETER

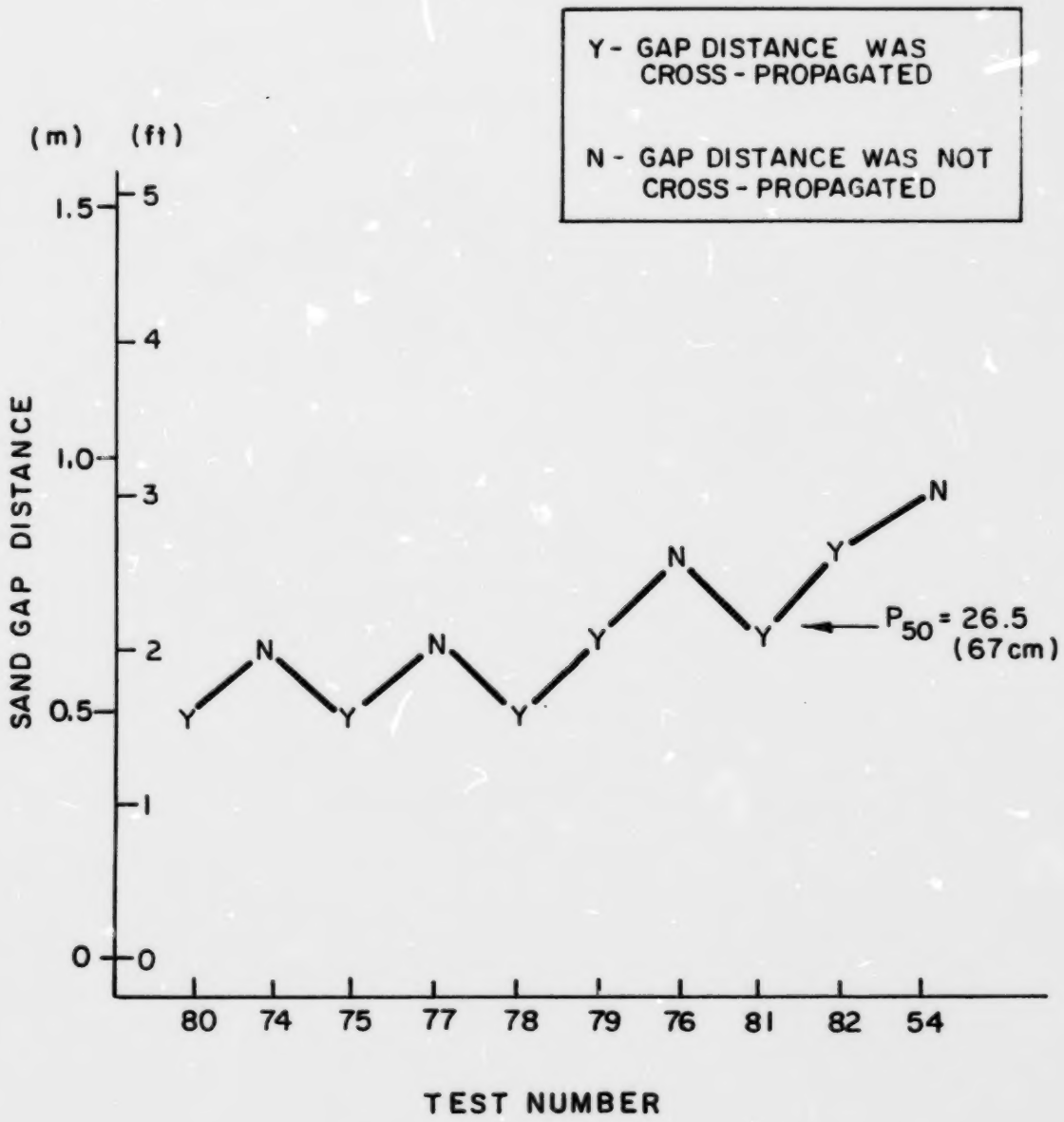

AN/FO – 150mm DIAMETER

APPENDIX G

"UP-AND-DOWN" RECEPTOR RESULT PLOTS FOR 90 MM AND 150 MM DIAMETER PRODUCT C WITH CAP AND CAST PRIMER IN THE RECEPTOR CHARGE

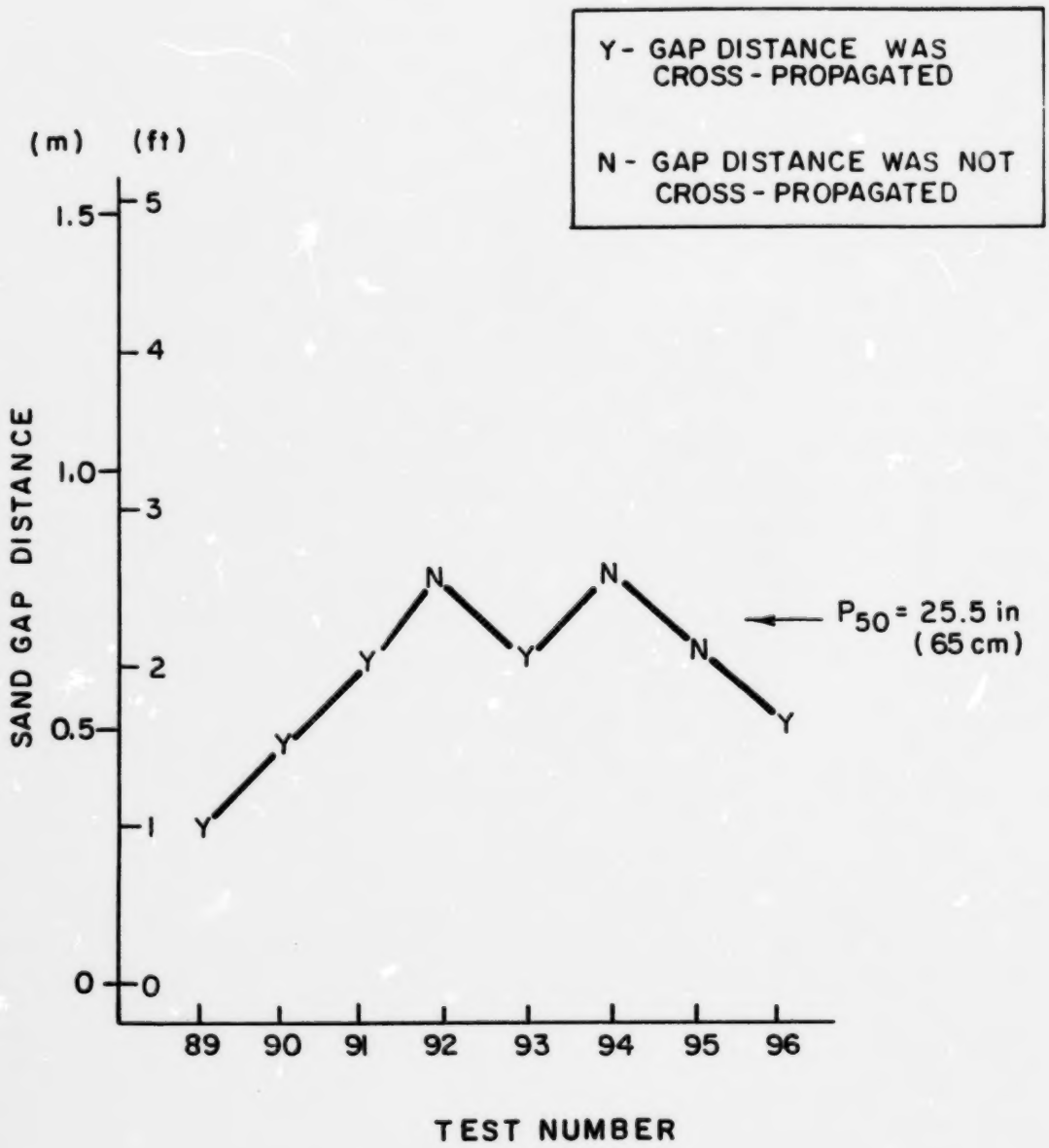

PRODUCT C — 90 mm DIAMETER WITH CAP AND PRIMER IN THE RECEPTOR CHARGE.

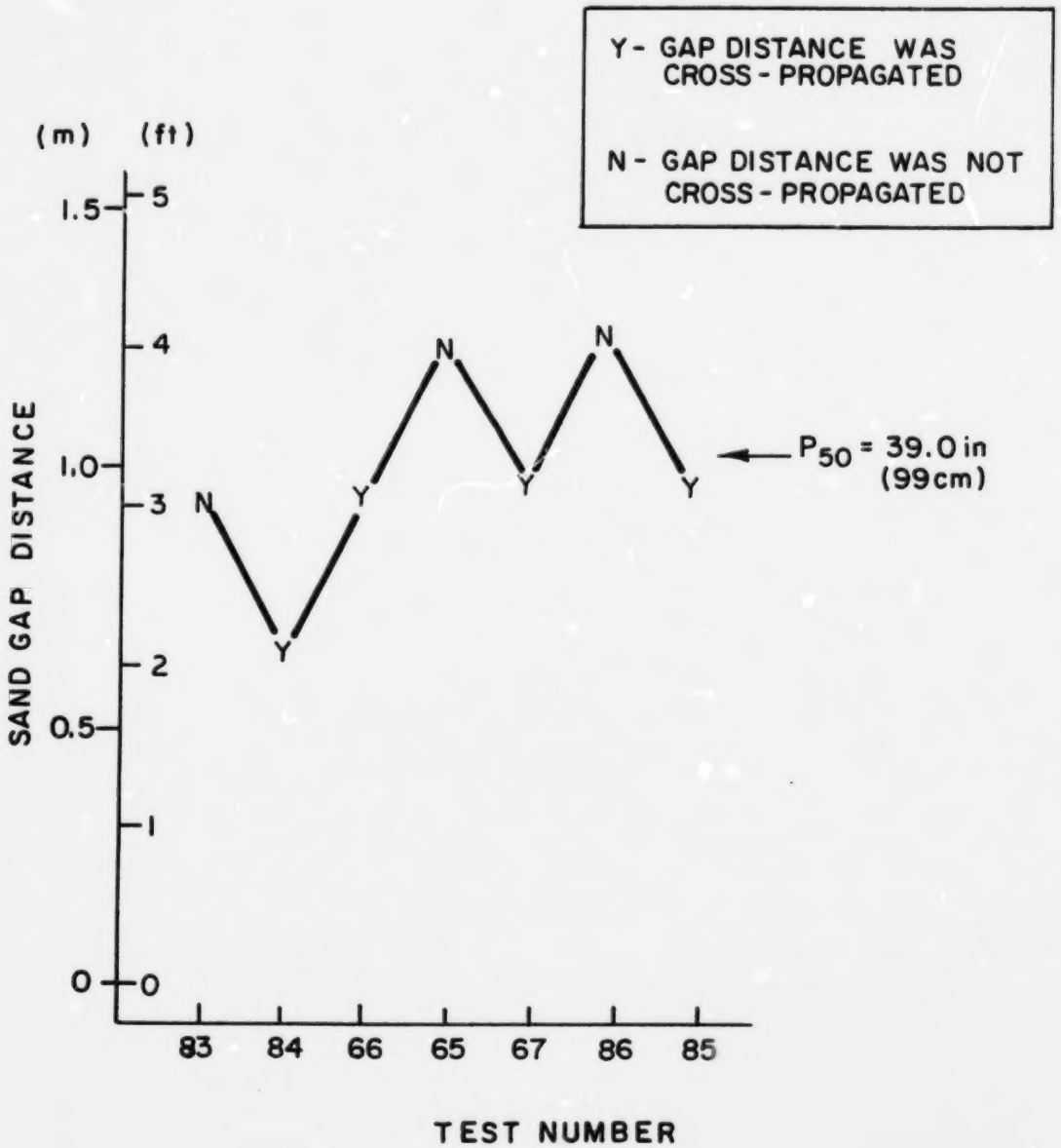

PRODUCT C — 150mm DIAMETER WITH CAP AND PRIMER IN THE RECEIVER CHARGE.

APPENDIX H

"UP-AND-DOWN" RECEPTOR RESULT PLOTS FOR 50 MM, 90 MM AND 150 MM DIAMETER CAP SENSITIVE PRODUCT D

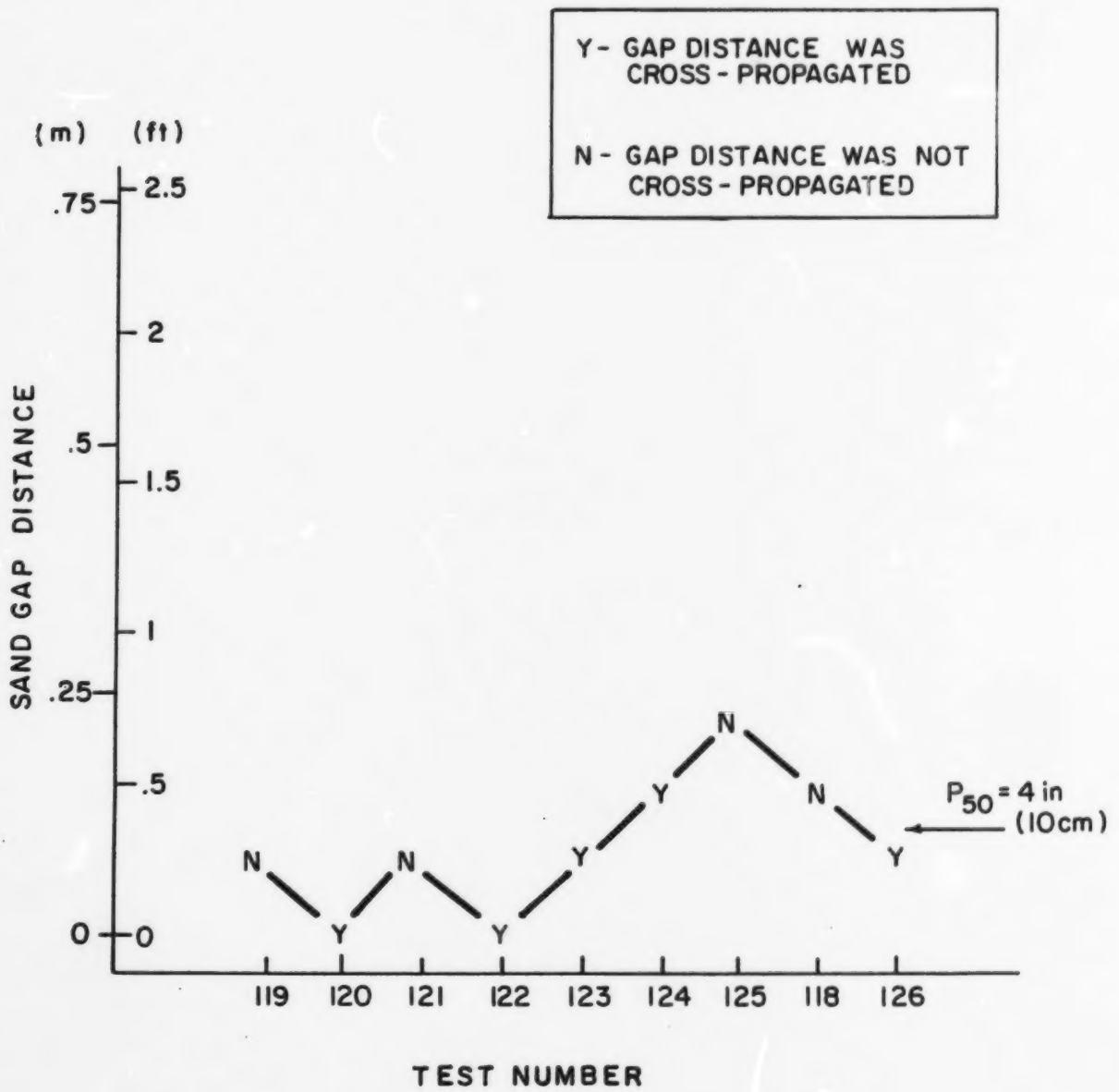

PRODUCT D — 50mm DIAMETER

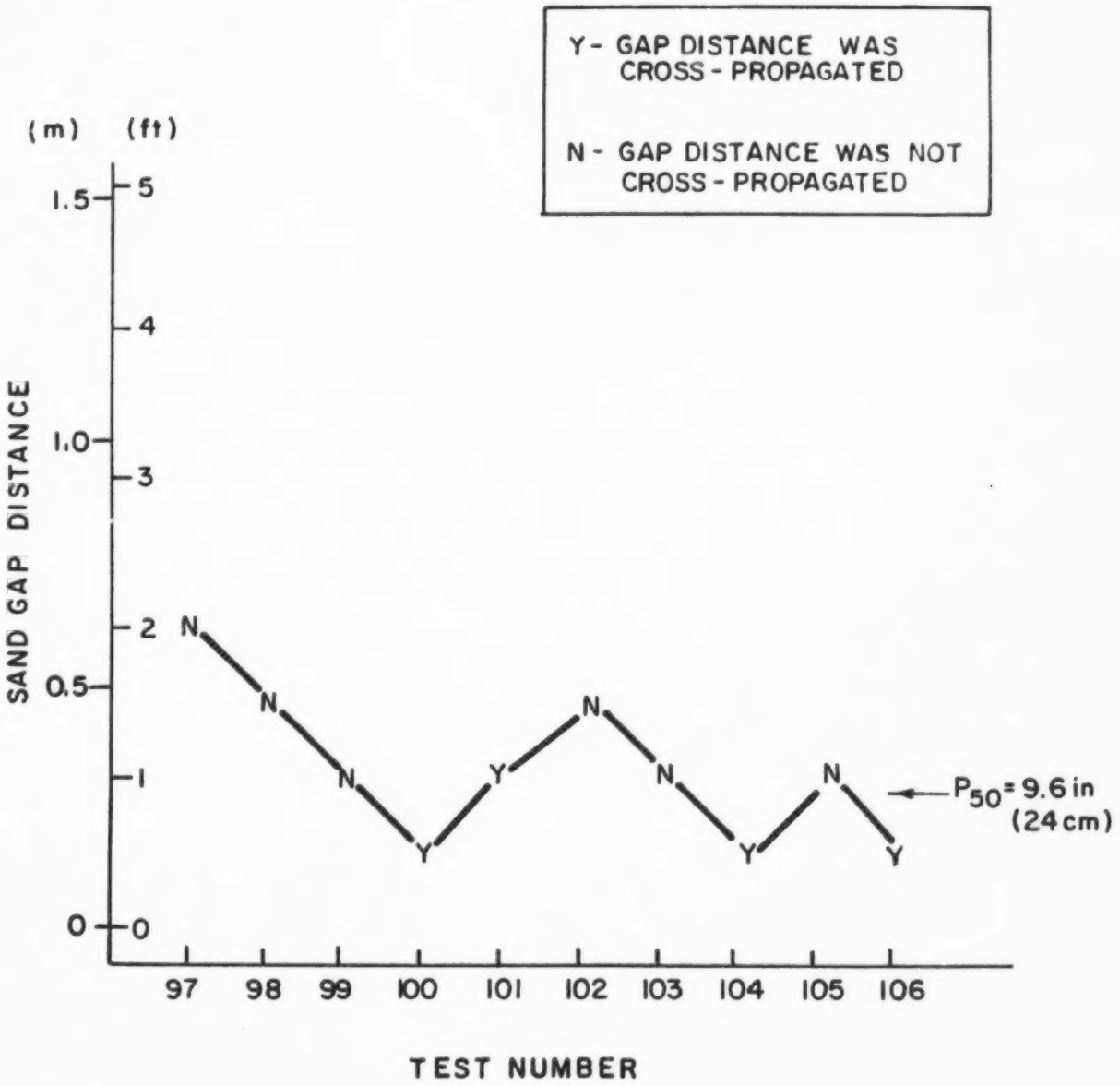

PRODUCT D — 90 mm DIAMETER

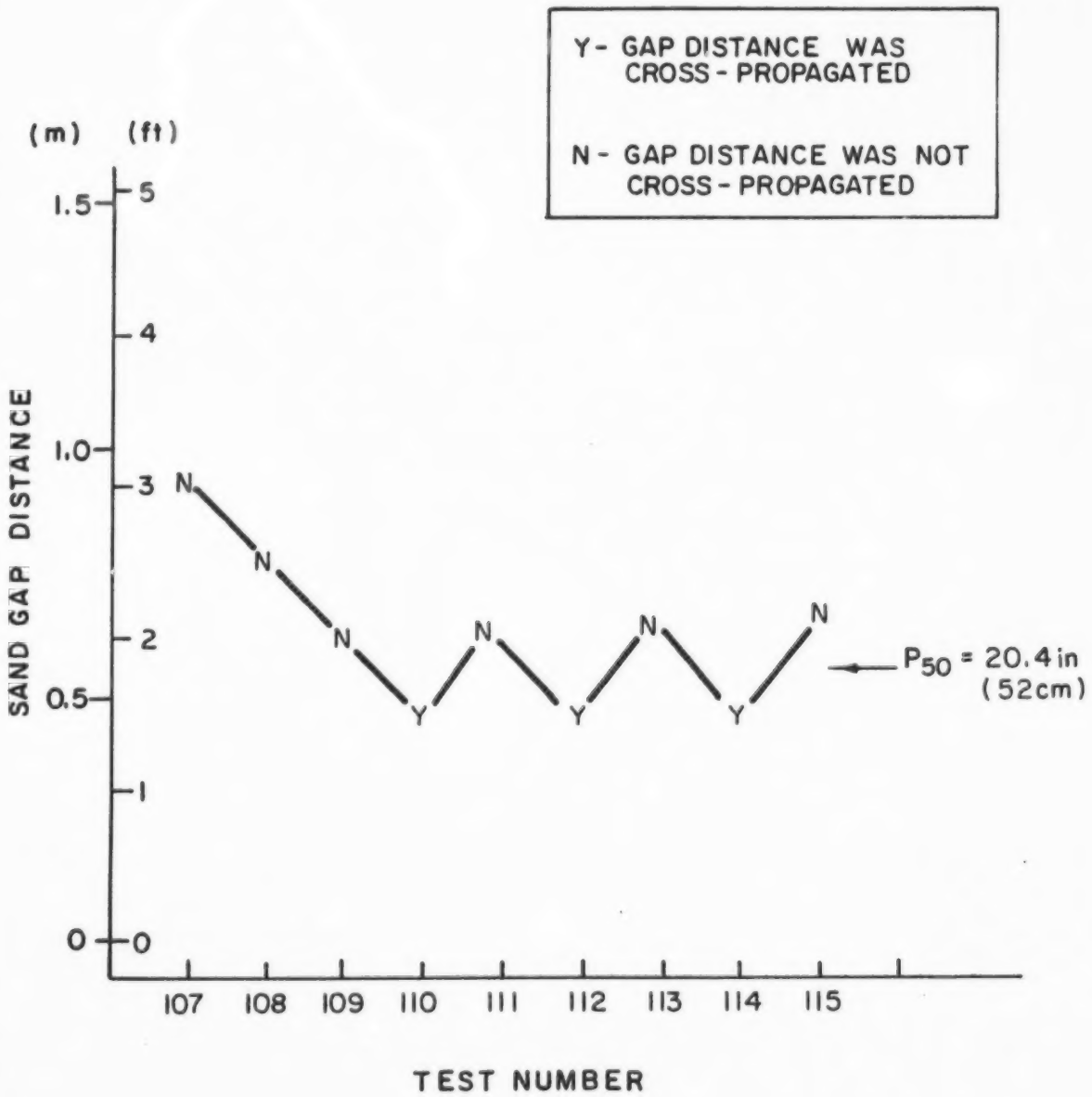

PRODUCT D – 150 mm DIAMETER